Cholinergic modulation of firing properties and IPSCs in rat nucleus accumbens shell

Katsuko Ebihara

Nihon University Graduate School of Dentistry,
Major in Dysphagia Rehabilitation

(Directors: Profs. Koichiro Ueda and Noriaki Koshikawa,
and Assoc. Prof. Masayuki Kobayashi)

Index

ABSTRACT

The nucleus accumbens (NAc) locates in the frontal part of the telencephalon and contributes to physiological functions such as fear, reward, learning and motor control. In addition, the NAc plays roles in induction of some pathophysiological symptoms, e.g., drug dependence and oral dyskinesia. The NAc contains three types of GABAergic inhibitory neurons and cholinergic interneurons. Medium spiny (MS) neurons are the principal and main projection neurons, and form local circuits of lateral inhibition in the NAc. They receive input from at least two GABAergic neurons, i.e., fast-spiking (FS) neurons and MS neurons themselves.

Despite representing less than 2% of local neurons, these cholinergic neurons exert dominant and powerful modulation of neural functions, including dopamine release, synaptic activity, and intrinsic electrophysiological properties of the NAc local circuit. Although the effects of acetylcholine on the action potential properties of NAc MS neurons have been studied, how intrinsic acetylcholine released from NAc cholinergic interneurons regulates the MS neuronal activity remains unknown. Additionally, physiological properties of inhibitory synaptic transmission differ depending on presynaptic neuron subtypes, and therefore, each synaptic connection may possibly exhibit contradictory modulation. However, the relationship between the cholinergic modulation of inhibitory postsynaptic currents (IPSCs) and the presynaptic cell subtypes is still an open issue. The present study performed whole-cell patch-clamp recordings from NAc shell slice preparations to examine the cholinergic modulation of (1) repetitive firing properties of MS neurons and (2) unitary inhibitory postsynaptic currents (uIPSCs).

The first series of experiments revealed that bath application of carbachol (10 μM) induced resting membrane potential depolarization accompanied by an increase in the voltage response to negative current injection. Furthermore, carbachol increased the rheobase and shifted the frequency-current curve towards the right. Repetitive spike firing of a cholinergic interneuron following positive current injection induced a similar increase in the rheobase, which delayed the action potential initiation in 38.9% MS neurons. In contrast, cholinergic interneuronal stimulation had little effect on the resting membrane potential in MS neurons.

In the second series of experiments, reciprocal regulation of inhibitory synaptic transmission by nicotinic and muscarinic receptors was investigated. Due to their high-frequency repetitive spike firing, FS neurons potently suppress postsynaptic MS neurons, showing large amplitude and low failure rate. In contrast, the recurrent collateral connections of MS neurons exhibit a lower connection rate and smaller amplitude of uIPSCs in comparison to the FS neurons. Thus, these MS/FS→MS connections are physiologically significant and it is necessary to discriminate the source of GABAergic inputs into the MS neurons. Bath application of carbachol suppressed uIPSCs amplitude by 58.3% in MS→MS connections and accompanied increases in the paired-pulse ratio and the failure rate, suggesting that acetylcholine reduces the release probability of GABA from the synaptic terminals of MS neurons. The carbachol-induced suppression of uIPSCs was antagonized by 100 μM atropine, and was mimicked by pilocarpine (1 μM) and acetylcholine (1 μM) but not nicotine (1 μM). In contrast, FS→MS connections showed that pilocarpine had little effect on the uIPSC amplitude, whereas either nicotine or acetylcholine facilitated the uIPSC amplitude with decreases in the failure rate and the paired-pulse ratio, suggesting that nicotine-induced uIPSC facilitation is mediated by presynaptic mechanisms. Miniature IPSC recordings support the hypotheses of the cholinergic presynaptic mechanisms.

Taken together with these findings, it is concluded that (1) bath application of carbachol reduced MS neuronal repetitive spike firing frequency, (2) acetylcholine released from a cholinergic interneuron is sufficient to suppress the repetitive spike firing of adjacent MS neurons, and (3) these suppressions occur via muscarinic receptors. Moreover, the inhibitory

synaptic transmissions in the NAc are modulated via (4) muscarinic receptors in MS→MS connections and (5) nicotinic receptors in FS→MS connections. Muscarinic and nicotinic receptors play differential roles in inhibitory synaptic transmission and GABA release, which depend on the presynaptic neuronal subtypes in the NAc shell.

CHAPTER I

Cholinergic interneurons suppress action potential initiation of medium spiny neurons in rat nucleus accumbens shell

Katsuko Ebihara, Kiyofumi Yamamoto, Koichiro Ueda, Noriaki Koshikawa, Masayuki Kobayashi. *Neuroscience* 236: 332-344, 2013.

Introduction

The nucleus accumbens (NAc), a rostroventromedial extension of the striatum, is involved in reward-related behaviors, drug abuse, psychosis, learning and motor control (Sharp et al., 1987, Koshikawa et al., 1990, Cools et al., 1995, Di Chiara, 2002, Nicola, 2007). The principal neurons in the NAc are medium spiny (MS) neurons, which are GABAergic and which project to the ventral pallidum and to the substantia nigra pars reticulata. Neural activities of the MS neurons are triggered by glutamatergic excitatory inputs from the prefrontal cortex and the medial thalamic nucleus. MS neuronal activities are modulated by dopamine that is released from the terminals of dopaminergic neurons from the ventral tegmental area, which suppresses the amplitude of the excitatory and inhibitory postsynaptic currents in the NAc (Nicola and Malenka, 1997).

In addition to dopamine, acetylcholine released from cholinergic interneurons in the NAc plays a critical role in the regulation of physiological function in the NAc. NAc cholinergic interneurons have large somata with characteristic electrophysiological profiles: large sag, rebound potential, and profound medium-duration afterhyperpolarization (mAHP). *In vivo* studies have demonstrated that cholinergic interneurons spontaneously fire with a regular interspike interval (Wilson et al., 1990), indicating that cholinergic inputs continuously effect NAc activity. Although cholinergic interneurons constitute <2% of the striatal neural population in the striatum (Phelps et al., 1985, Rymar et al., 2004, Threlfell and Cragg, 2011), their axons are densely distributed throughout the NAc (Zhou et al., 2003), which implies the potent modulation of NAc function by acetylcholine. Indeed, a recent study using optogenesis has demonstrated that the activation of NAc cholinergic interneurons suppresses the spontaneous firing of MS neurons in freely moving rats (Witten et al., 2010).

Cholinergic modulation of neural activity, including the modulation of intrinsic membrane properties and synaptic transmission of MS neurons, has been well studied by whole-cell patch-clamp recording in striatal slice preparations. Acetylcholine depolarizes the resting membrane potential and increases input resistance via M_1 receptors in the striatal MS neurons (Hsu et al., 1996). Cholinergic muscarinic agonists facilitate the spike firing of MS neurons by increasing input resistance and changing the subthreshold membrane conductance (Galarraga et al., 1999, Zhang and Warren, 2002, Perez-Rosello et al., 2005). In addition to its cholinergic effects on intrinsic membrane properties, acetylcholine also suppresses the release of glutamate and GABA in the terminals of MS neurons (Hsu et al., 1995, Calabresi et al., 2000).

In spite of the abundant evidence for the cholinergic modulation of MS neural functions, cholinergic effects on the MS neurons of the NAc have been less well reported. This surprising oversight might be attributable to the fact that the striatum and the NAc consist of similar cell subtypes, i.e., MS, fast spiking, persistent, low-threshold spiking, cholinergic neurons (Kawaguchi et al., 1995). In addition, both the striatum and the NAc receive dense dopaminergic and cholinergic projections. However, differences between the dopamine-related biochemical properties of the MS of the dorsal striatum and the NAc have been reported (Nicola and Malenka, 1998, Gulley et al., 2002, Stuber et al., 2010, Ma et al., 2012).

Morphologically, MS neurons of the NAc have smaller somatic size and fewer dendrites than those of the dorsal striatum (Ma et al., 2012). Furthermore, their intrinsic electrophysiological properties are also different; the MS neurons of the NAc have smaller rheobases, larger input resistance, different decay time constants, and different Ih amplitudes (Ma et al., 2012). This evidence suggests that the previously reported electrophysiological evidence from the striatum may not be applicable to the NAc.

Although Zhang and Warren (2002) have reported that carbachol application increases repetitive firing frequency in MS neurons of the NAc, the concentration of carbachol is relatively high (50 μM), which also induces substantial depolarization (+21 mV) of the resting membrane potential. Therefore, in the present study, the cholinergic regulation of intrinsic electrophysiological properties of NAc MS neurons was re-examined under physiological conditions (i.e., examining the effects not only of lower concentrations of carbachol but also of the electrical stimulation of a cholinergic neuron in NAc slice preparation).

Methods

All experiments were performed in accordance with the National Institutes of Health Guide for the Care and Use of Laboratory Animals and were approved by the Institutional Animal Care and Use Committee of Nihon University. All efforts were made to minimize the number of animals used and their suffering.

Slice preparations

The techniques for preparing and maintaining rat cortical slices *in vitro* were similar to those described previously (Kobayashi et al., 2012); hence, only a brief account of the methods employed will be given here. Wistar rats of either sex, aged from postnatal day 20 to 30, were deeply anesthetized with sodium pentobarbital (75 mg/kg i.p.) and decapitated. Tissue blocks including the NAc shell were rapidly removed and stored for 3 min in ice-cold modified artificial cerebrospinal fluid (ACSF) with the following composition (in mM): 230 sucrose, 2.5 KCl, 10 $MgSO_4$, 1.25 NaH_2PO_4, 26 $NaHCO_3$, 0.5 $CaCl_2$, and 10 D-glucose. Coronal slices were cut at 350 μm thickness using a microslicer (Linearslicer Pro 7, Dosaka EM, Kyoto, Japan). The slices were incubated at 32°C for 40 min in a submersion-type holding chamber that contained 50% modified ACSF and 50% normal ACSF (pH 7.35-7.40). Normal ACSF contained the following (in mM): 126 NaCl, 3 KCl, 2 $MgSO_4$, 1.25 NaH_2PO_4, 26 $NaHCO_3$, 2.0 $CaCl_2$, and 10 D-glucose. Modified and normal ACSF were continuously aerated with a mixture of 95% O_2 / 5% CO_2. The slices were then placed in normal ACSF at 32°C for 1 h and were thereafter maintained at room temperature until recording.

Whole-cell patch-clamp recording

The slices were transferred to a recording chamber and were continuously perfused with normal ACSF at a rate of 1.5-2.0 ml/min. Single or multiple whole-cell patch-clamp recordings were obtained from MS neurons and from cholinergic interneurons from the NAc shell with a microscope equipped with Nomarski optics (BX51, Olympus, Tokyo, Japan) and an infrared-sensitive video camera (Hamamatsu Photonics, Hamamatsu, Japan). The distance between the MS neurons and the cholinergic interneurons, thus the distance between the center of their somata, was < 100 μm. Electrical signals were recorded with amplifiers (Axoclamp 700B, Axon Instruments, Foster City, CA), digitized (Digidata 1440A, Axon Instruments), observed on-line and stored on a computer hard disk using Clampex (pClamp 10, Axon Instruments).

The composition of the pipette solution used for recordings from the MS and cholinergic neurons was as follows (in mM): 135 potassium gluconate, 5 KCl, 5 *N*-(2-hydroxyethyl)piperazine-*N'*-2-ethanesulfonic acid (HEPES), 20 biocytin, 5 EGTA, 2 $MgCl_2$, 2 magnesium adenosine triphosphate (ATP), and 0.3 sodium guanosine triphosphate (GTP). The pipette solution had a pH of 7.3 and an osmolarity of 300 mOsm. The liquid junction potential for the current-clamp and voltage-clamp recordings was -9 mV, and the voltage was corrected accordingly. Thin-wall borosilicate patch electrodes (2-5 MΩ) were pulled from a Flaming-Brown micropipette puller (P-97, Sutter Instruments, Novato, CA).

The recordings were obtained at 30-31°C. The seal resistance was > 5 GΩ, and only the data obtained from electrodes with access resistance of 6-20 MΩ and < 20% change during the recordings were included in this study.

Voltage responses were recorded via the application of hyper- and depolarizing current pulse injections to examine the basic electrophysiological properties, including input resistance, single spike kinetics, voltage-current relationships, rheobase, repetitive spike firing patterns and firing frequency. Membrane currents and potentials were low-pass filtered at 5-10 kHz and digitized at 20 kHz. The following drugs were added directly to the perfusate: carbachol (1-30 μM), pirenzepine (10 μM), and atropine (100 μM). In the experiment to

examine the effects of intrinsic acetylcholine release on MS neuronal spike firing, long depolarizing current pulses (500 ms, 0.2 Hz) were injected into a cholinergic interneuron in the same timing of current injection applied to MS neurons. The depolarizing currents to cholinergic interneurons were set at the intensity that induced repetitive spike firing at 10-20 Hz.

Data analysis

Input resistance was calculated from the relationship between the injected current intensity (-20 to -80 pA) and the steady-state voltage response (> 250 ms). The amplitude of the ramp depolarizing potential in response to the maximal current that did not elicit action potential was obtained by subtraction of the membrane potential at 50 ms from that at ~500 ms. The action potential threshold was assigned as the potential at which the third derivative of the membrane potential changed sign from negative to positive (Takei et al., 2010; Fig. 1A,B). The amplitudes of the action potential and mAHP were measured from the positive and negative peaks of the action potential threshold, respectively. The repetitive spike firing properties were evaluated by measuring the slope of a least-squares regression line in a plot of the number of spikes versus the amplitude of the injected current, up to approximately 750 pA (f/*I*). The resting membrane potential during application of carbachol, or cholinergic neuronal stimulation, was not adjusted to that in control.

The data are presented as the means ± standard error of the means (SEM). Comparisons between the MS neurons and cholinergic interneurons were made using Student's *t*-test. Comparisons between the control and carbachol application were made using paired *t*-tests. Typically, recordings made 15 min after carbachol application were used to quantify the effects of carbachol on the electrophysiological properties. Similarly, comparisons between the control and cholinergic neuronal stimulations were made using paired *t*-tests. Spearman Rho test was used to examine the relationship between the cholinergic effects on the rheobase and the distance between MS and cholinergic neurons. The level of $P < 0.05$ was adopted to indicate significance.

Histology

To visualize biocytin-labeled neurons after whole-cell patch-clamp recording, the slices were fixed, stored, and processed using a whole-mount protocol (Fig. 1; Kobayashi et al., 2012). The slices were rinsed in 0.5% Triton X-100 and 0.1 M glycine in 0.1 M phosphate buffer and then incubated with fluorophores Alexa 594 streptavidin (5 mg/μL, Molecular Probes, Eugene, OR) in blocking solution overnight. The slices were rinsed in 0.5% Triton X-100 and 0.1 M glycine in 0.1 M phosphate buffer, mounted on slides, and cover-slipped with Vectashield (Vector Laboratories). The slices were examined, and images were obtained with a confocal microscope (FV-1000, Olympus, Tokyo, Japan). Unless stated otherwise, all chemicals were purchased from Sigma-Aldrich (St. Louis, MO).

Results

Table 1 shows the basic electrophysiological properties of MS neurons and cholinergic interneurons in the NAc shell. The following criteria were used to select neurons: stable resting negative membrane potentials of more than –60 mV and overshoot action potentials. MS neurons were identified using the following criteria: (1) small soma, (2) deep resting membrane potential, (3) high input resistance, and (4) ramp potential in response to depolarizing current pulses (Fig. 2A). Cholinergic interneurons have large somata (Fig. 1), and they frequently showed profound afterhyperpolarization and sag with rebound action potentials responding to hyperpolarizing current injection (Fig. 2B).

Table 1. Intrinsic electrophysiological properties of MS and cholinergic neurons in the NAc

	MS neurons		Cholinergic interneurons	
	Mean ± S.E.M.	n	Mean ± S.E.M.	n
Vm† (mV)	-80.7 ± 0.9**	52	-75.3 ± 1.2	24
Input resistance (MΩ)	221.1 ± 15.1*	39	170.4 ± 12.4	20
Action potential amplitude (mV)	71.2 ± 2.3	50	70.3 ± 2.5	17
Ramp (mV)	6.4 ± 0.4**	50	3.5 ± 0.7	15
Action potential threshold	-47.0 ± 1.2	41	-49.5 ± 1.6	18
mAHP†† amplitude (mV)	13.7 ± 1.3	52	13.1 ± 1.6	17
f/I slope (Hz/pA)	0.206 ± 0.02*	52	0.126 ± 0.01	16

†Resting membrane potential; ††Medium-duration afterhyperpolarization; *: $P < 0.05$, **: $P < 0.01$ (Student's *t*-test).

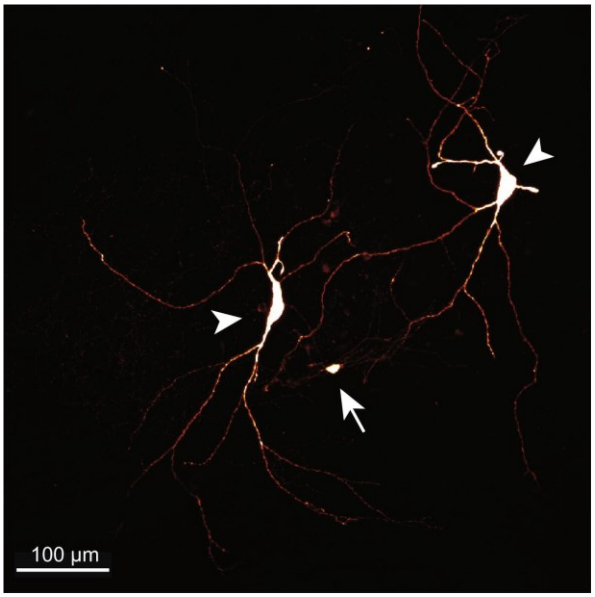

Figure 1. Biocytin-labeling of a medium spiny (MS; arrow) and two cholinergic neurons (arrowheads) in the nucleus accumbens shell.

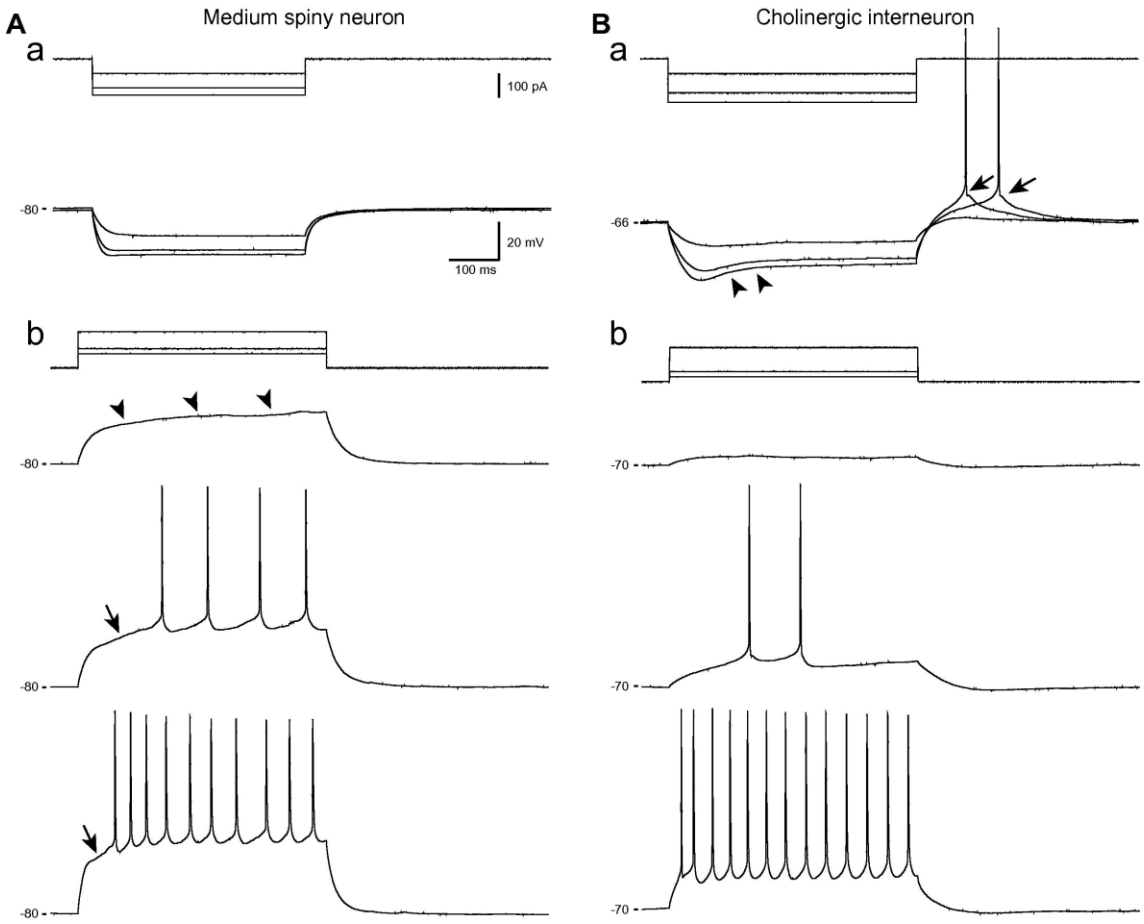

Figure 2. Passive membrane and spike firing properties of MS and cholinergic neurons. ***A.*** Representative traces of an MS neuron. Hyperpolarizing (***a***) and depolarizing (***b***) responses to long current pulse injection are shown. Arrowheads and arrows indicate a ramp depolarized potential and temporal lags before the 1st spike initiation, respectively. ***B.*** Hyperpolarizing (***a***) and depolarizing (***b***) responses to the long current pulse injection of a cholinergic interneuron. Initial membrane hyperpolarization is followed by the characteristic depolarizing sag (arrowheads) and rebound action potentials (arrows). The resting membrane potentials are shown on the left of each trace.

Carbachol depolarizes resting membrane potential

Bath application of carbachol (10 μM) depolarized the resting membrane potential of MS neurons with an increase in the voltage response to hyperpolarizing current pulse injection (Fig. 3A-C). These carbachol-induced effects on subthreshold responses were reversible. The lower concentration of carbachol (1 μM) induced only a slight depolarization (Fig. 3D). These depolarizing effects of carbachol were blocked by pre-application of pirenzepine, an M_1 muscarinic receptor antagonist (10 μM; data not shown).

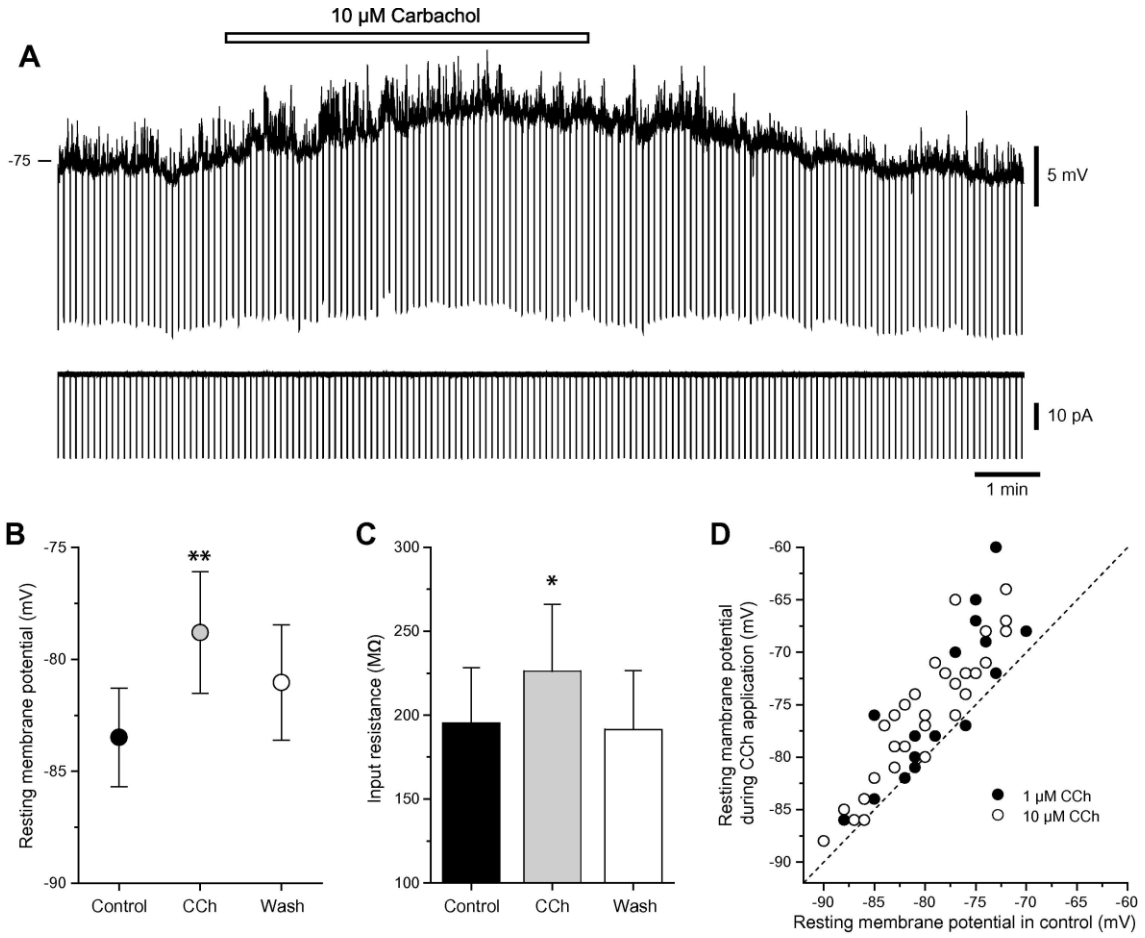

Figure 3. Effects of carbachol on the resting membrane potential and hyperpolarizing potentials responding to negative current pulse injection. ***A.*** An example of the depolarizing resting membrane potential during carbachol application recorded from an MS neuron. Hyperpolarizing responses to negative current injection (lower) were increased. ***B.*** Summary of the effect of carbachol on the resting membrane potential. ***C.*** Summary of the effect of carbachol on input resistance. ***D.*** Relationship between the resting membrane potential and its change caused by the application of 1 and 10 μM carbachol. The identical line is indicated by dots. *: $P < 0.05$, **: $P < 0.01$, paired *t*-test.

Carbachol suppresses repetitive spike firing

Carbachol suppressed the frequency of repetitive spike firing of the MS neurons in a dose-dependent manner (Fig. 4A-C). Although the application of carbachol slightly depolarized the resting membrane potential, carbachol reduced the frequency of action potentials responding to depolarizing long current pulse injection. As a result, the f/*I* curves shifted towards the right, which indicated an increase in the rheobase. The mean increase in the rheobase induced by 1 μM carbachol was 28.6 ± 6.5% (n = 16; $P < 0.01$, paired *t*-test). The slope of the regression line fitted to f/*I* curves was little affected by carbachol (0.231 ± 0.024 to 0.217 ± 0.028 Hz/pA by 1 μM carbachol and 0.221 ± 0.025 to 0.216 ± 0.027 Hz/pA by 10 μM carbachol; Fig. 4D,E).

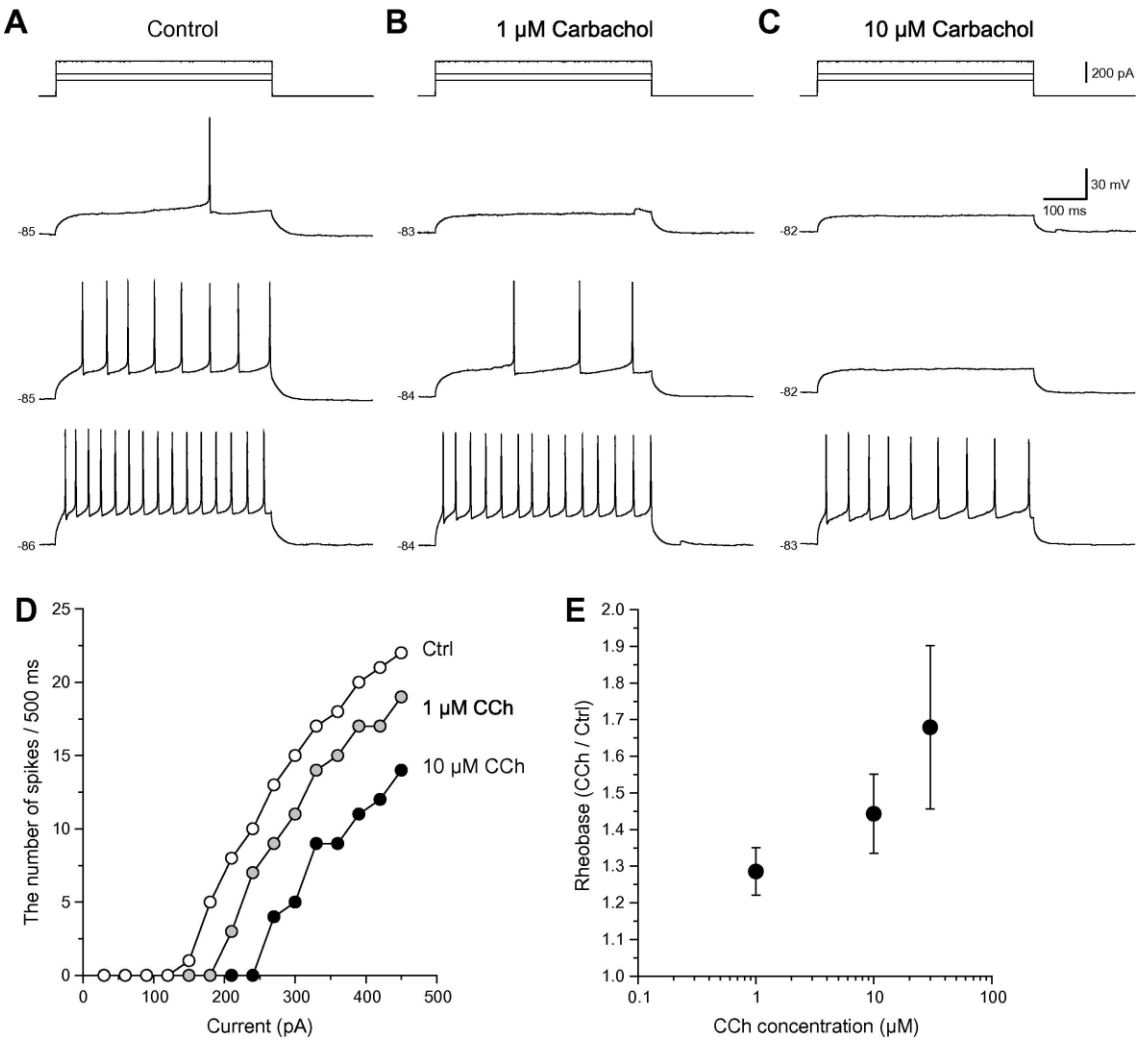

Figure 4. Suppressive effects of carbachol on repetitive spike firing. ***A, B*** and ***C.*** Repetitive spike firing in response to long depolarizing pulses in control (***A***) and with the application of 1 μM (***B***) and 10 μM carbachol (***C***). ***D.*** The f/*I* relationship in the neuron shown in ***A-C*** before (open circles) and during 1 μM (gray circles) and 10 μM (filled circles) carbachol application. ***E.*** The dose-dependent increase in rheobase caused by carbachol (1 μM, n = 17; 10 μM, n = 24; 30 μM, n = 9).

It is reported that cholinergic activation increases dopamine release in the NAc (Kitamura et al., 1999), and therefore, the carbachol-induced increase in the rheobase might be mediated by modulating dopaminergic system. To explore this possibility, the effects of carbachol on the rheobase were examined in the presence of dopaminergic receptor antagonists.

Carbachol (1 μM) was applied in combination with 30 μM SCH 23390, a D_1-like receptor antagonist, and 10 μM sulpiride, a D_2-like receptor antagonist. Under blockade of these dopaminergic receptors, carbachol still similarly increased the rheobase by 33.6 ± 13.3 pA (n = 12, $P < 0.05$, paired *t*-test), suggesting that carbachol is likely to increase the rheobase directly (Fig. 5A and B).

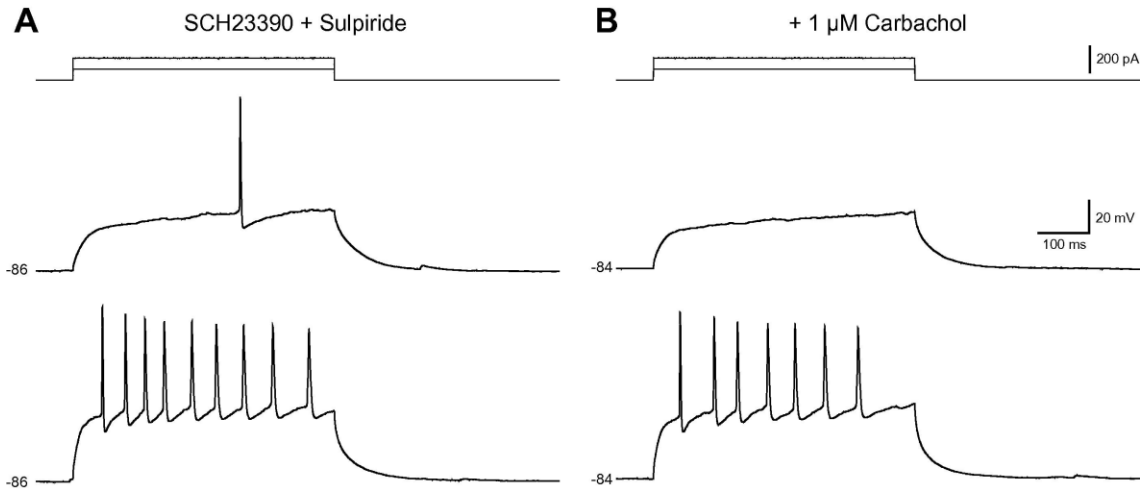

Figure 5. Effects of carbachol on repetitive firing properties under application of dopaminergic receptor antagonists. ***A.*** Repetitive spike firing in response to long depolarizing pulses with the application of 30 μM SCH 23390 and 10 μM sulpiride. ***B.*** Carbachol (1 μM) in combination with SCH 23390 and sulpiride suppressed spike firing.

The mechanisms of carbachol-induced increase in rheobase

In general, the depolarization of the resting membrane potential facilitates spike induction, and the increase in input resistance enhances the voltage response, which also results in facilitates spike firing responding to depolarizing current pulse injection. However, carbachol increased the rheobase, which decreased the spike firing frequency responding to a depolarizing current pulse injection. To elucidate the mechanisms underlying this discrepancy, the voltage responses to depolarizing current pulse injections were analyzed.

Fig. 6A shows an example of the voltage responses to the rheobase in the control; this response induced a single action potential after ramp depolarizing potential (arrowheads). In contrast to the control, the voltage response during carbachol application showed smaller amplitude of the ramp depolarizing potential (arrow), and as a result, an action potential was not triggered in spite of the depolarization of the resting membrane potential from -79 to -73 mV. The mean decrease in the amplitude of the ramp depolarizing potential by 1 μM carbachol was 2.8 ± 0.9 mV (n = 16; $P < 0.05$, paired *t*-test). The larger current injection evoked repetitive spike firing during carbachol application (Fig. 6B). In comparison to the traces collected from the control, which showed a similar firing frequency, the threshold and the amplitude of mAHP were almost comparable. In the same neuron as shown in Fig. 6A and B, carbachol induced larger potentials in response to hyperpolarizing current pulse injection. Fig. 6D summarizes the subthreshold voltage responses in the control and during carbachol application in the same cell. Typically, MS neurons exhibit a V/*I* relationship with outward rectification. Therefore, the present results suggest that carbachol enhances hyperpolarizing voltage responses but decreases depolarizing responses.

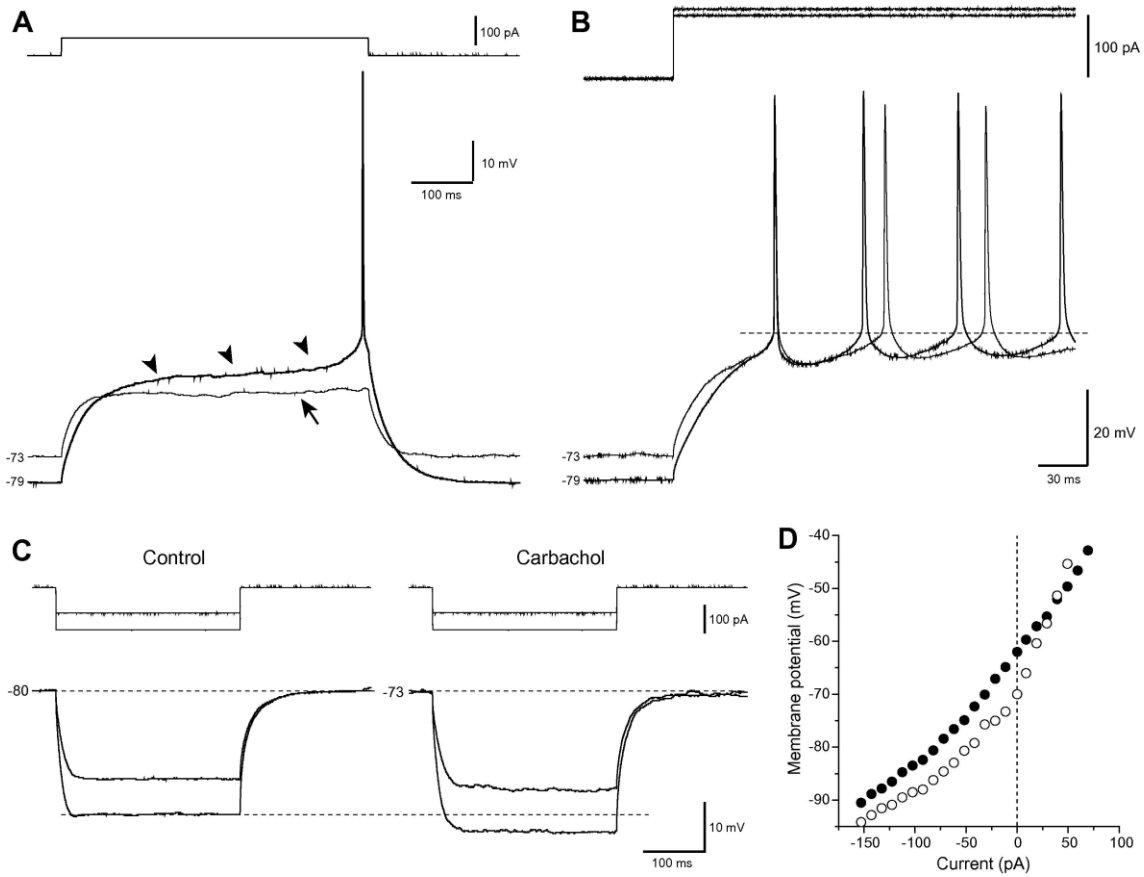

Figure 6. Contradictory effects of carbachol (1 μM) on depolarizing and hyperpolarizing potentials. ***A.*** Superimposed voltage responses to the depolarizing current injection that induced the threshold response in the control (black). Carbachol (gray) depolarized the resting membrane potential and suppressed the slowly depolarizing potential in the control (arrowheads). ***B.*** Suprathreshold responses in the control (black) and during carbachol application (gray) are superimposed. Note that little change in the spike threshold occurred. ***C.*** Carbachol enhanced the hyperpolarized response in the same cell presented in ***A*** and ***B***. ***D.*** Current-voltage relationship in the control (open circles) and during carbachol application (filled circles).

Acetylcholine release from cholinergic interneuron suppresses spike firing

Cholinergic interneurons in the NAc are considered to be the main source of acetylcholine for MS neurons. However, it is still unknown whether the activities of cholinergic interneurons definitively regulate neuronal firing of MS neurons in the NAc. The present study showed that bath application of carbachol suppressed MS neuronal firing in the NAc; the effects of cholinergic interneuronal excitation on adjacent MS neuronal activity were also examined by performing multiple whole-cell patch-clamp recordings, which enabled to record MS neuronal activity before and during the repetitive firing of cholinergic interneurons.

Fig. 7 shows an example of a quad whole-cell patch-clamp recording from one cholinergic neuron and 3 MS neurons in the NAc. In the control, an f/*I* test was performed in 3 MS neurons without stimulation of the cholinergic interneurons (Fig. 7C). To avoid the spontaneous firing of the cholinergic interneuron adjacent to the recorded MS neurons, the resting membrane potential of the cholinergic interneuron was hyperpolarized by direct current injection. After this control recording, an f/*I* test was performed in the same MS neurons in combination with cholinergic interneuronal stimulation (Fig. 7D). There was a slight variability in the number of action potentials during the depolarizing current pulses, but in most of the trials, 5 spikes per 500 ms pulses were observed. Cholinergic neuronal

stimulation caused a reduction in the spike firing in the MS1 and MS2 neurons but not in the MS3 neuron (Fig. 7C and D). The characteristic suppression profile of carbachol, i.e., reduction of the slowly depolarizing potential (Fig. 6A), was observed in the MS1 and MS2 neurons (Fig. 7E), suggesting that intrinsic acetylcholine release caused similar effects to those of the carbachol application, partly because of the MS neurons adjacent to the cholinergic interneuron. In this case, the resting membrane potential of the MS2 neuron showed a slight depolarization, but the MS1 neuron remained unchanged. No fast synaptic transmission from the cholinergic neuron to the MS neurons was observed.

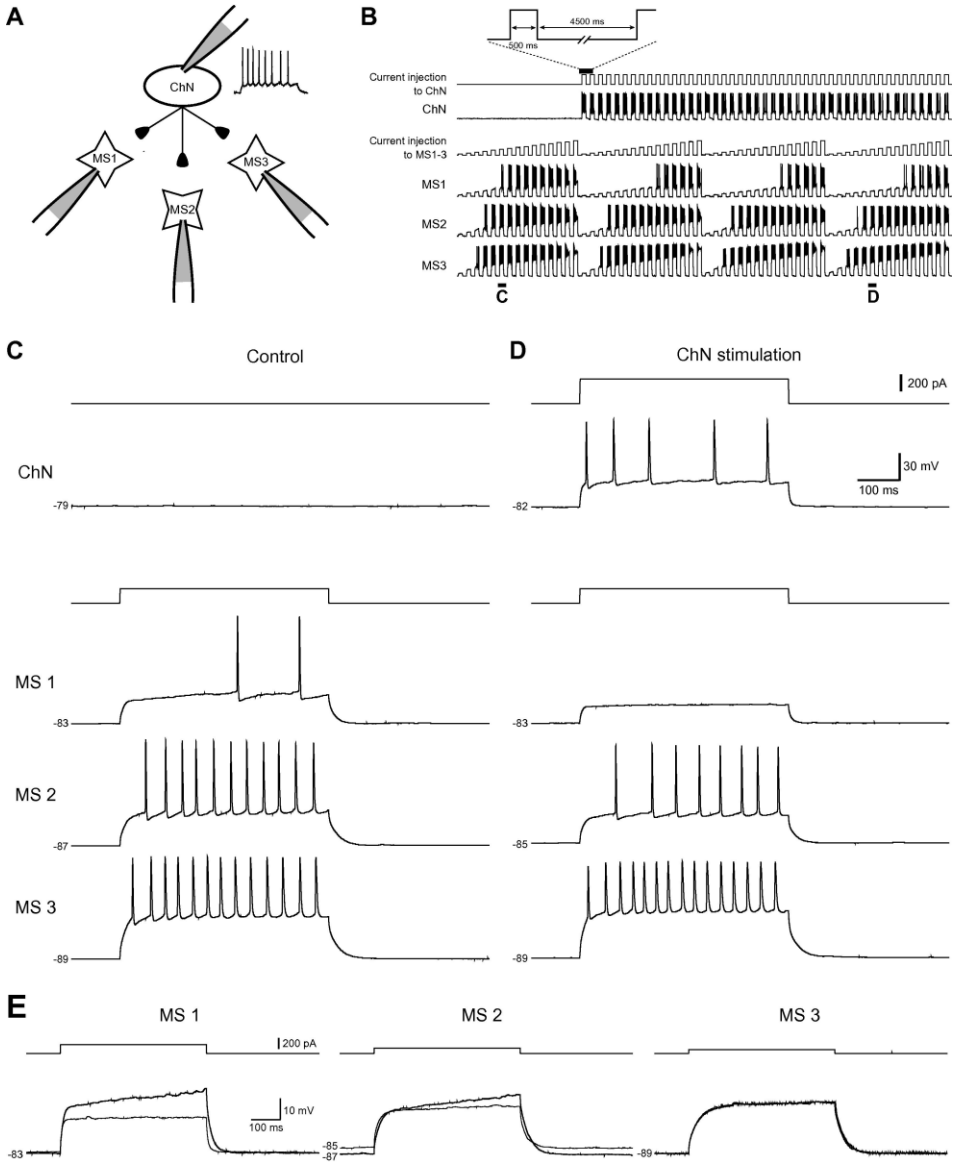

Figure 7. Suppressive effects of a recruited cholinergic neuron on repetitive spike firing in MS neurons. ***A.*** Quad whole-cell patch-clamp recording was performed using three MS neurons (MS1, MS2, and MS3) and a cholinergic neuron (ChN). ***B.*** Repetitive depolarizing current pulses (15 pulses with Δ20 pA) were applied to three MS neurons (the middle current trace). In the control, the cholinergic neuron was not stimulated (the early phase of recording). After recording the control, the constant depolarizing current pulses (inset) were injected in combination with stimulation of the MS neurons. ***C.*** Spike firing responses of MS1-3 neurons without cholinergic spike firing during the period indicated by line ***C*** in panel ***B***. ***D.*** Spike firing responses of MS1-3 neurons with cholinergic spike firing during the period indicated by line ***D*** in panel ***B***. Note the suppressive effects of the firing responses in MS1 and MS2 neurons. ***E.*** Subthreshold membrane potentials of three MS neurons in ***B-D*** with (gray traces) or without the cholinergic neuronal firing (black traces). Note that the depolarizing ramp response was abolished by cholinergic activation in MS1 and MS2 neurons.

In total, the present study simultaneously recorded 36 MS neurons with adjacent cholinergic interneurons. In 22/36 MS neurons (61.1%), there was a significant change in spike firing frequency, and 14/36 (38.9%) neurons showed an increase in the rheobase. The interval between the first spike of a MS neuron and the preceding spike in a cholinergic interneuron was 59.8 ± 11.3 ms (ranged from 1.2-219.2 ms; n = 31). There was no significant relationship between the effect on the rheobase and the distance between the MS and cholinergic neurons (Fig. 8, $P > 0.2$, Spearman Rho test), suggesting that cholinergic axons broadly distribute at least 100 μm from the cholinergic neuronal soma in the slice preparations (Kawaguchi, 1993). In addition, the present study performed statistical analysis to examine the relationship between the effect on the rheobase and the resting membrane potential/input resistance/rheobase, which may reflect the difference between the MS neurons expressing D_1 and D_2 receptors (Gertler et al., 2008, but also see Taverna et al., 2008; Ma et al., 2012). There were no significant correlation between the effect on the rheobase and these parameters ($P > 0.2$, Spearman Rho test).

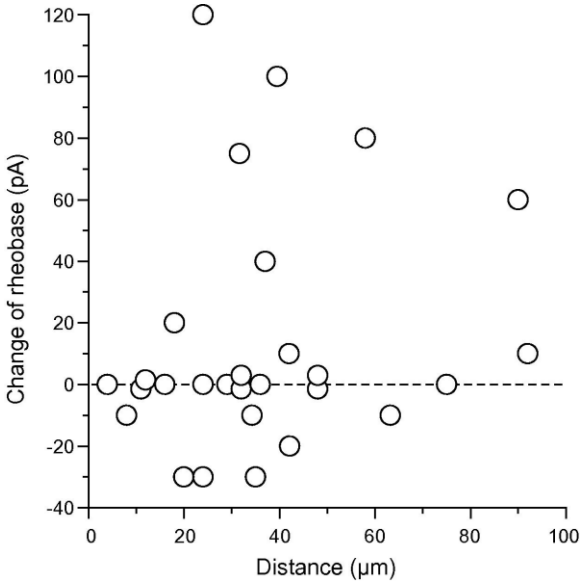

Figure 8. Relationship between the change in rheobase and the distance between the MS and cholinergic neurons.

Intrinsic acetylcholine-induced suppression of spike firing is blocked by atropine

In those multiple whole-cell patch-clamp recordings, 38.9% of the MS neurons exhibited characteristic suppression of the slow depolarizing potential, suggesting that intrinsic acetylcholine suppresses MS spike firing. However, note that a few MS neurons showed little effect on their spike firing during cholinergic interneuronal activation. To avoid the argument that other unknown factors besides acetylcholine might modulate the spike firing of MS neurons, the present study examined the effects of atropine, a non-selective muscarinic antagonist, on those MS neurons that exhibited firing suppression in response to the activation of cholinergic interneurons.

Figure 9 shows an example of a pair recording from a cholinergic and an MS neuron, both of which showed the atropine-dependent recovery of MS spike firing. In the control, an f/*I* test was performed in the MS neuron without activation of the cholinergic interneuron (Fig. 9B and Ca). Then, an f/*I* test was performed in combination with spike induction of the cholinergic interneuron (Fig. 9B and Cb). The acceleration of spike firing in the cholinergic interneuron induced more potent suppression of spike firing in the MS neuron (Fig. 9Cc). A pause in the cholinergic interneuronal stimulation partially recovered spike firing in the MS

neuron (data not shown), and subsequent application of atropine strengthened the firing recovery of the MS neurons (Fig. 9Cd). Finally, cholinergic interneuronal stimulation during the application of atropine had little effect on the spike firing frequency of the MS neuron (Fig. 9Ce).

The present study recorded five pairs of cholinergic and MS neurons to examine the effects of atropine, and under application of atropine, there was no significant effect of cholinergic interneuronal stimulation on the rheobase of MS neurons (72.9 ± 15.6 pA to 62.5 ± 14.5 pA, n = 5; $P > 0.2$, paired *t*-test). Therefore, it is likely that spike induction in cholinergic interneurons releases acetylcholine and suppresses neuronal firing of a part of MS neurons by activation of muscarinic receptors.

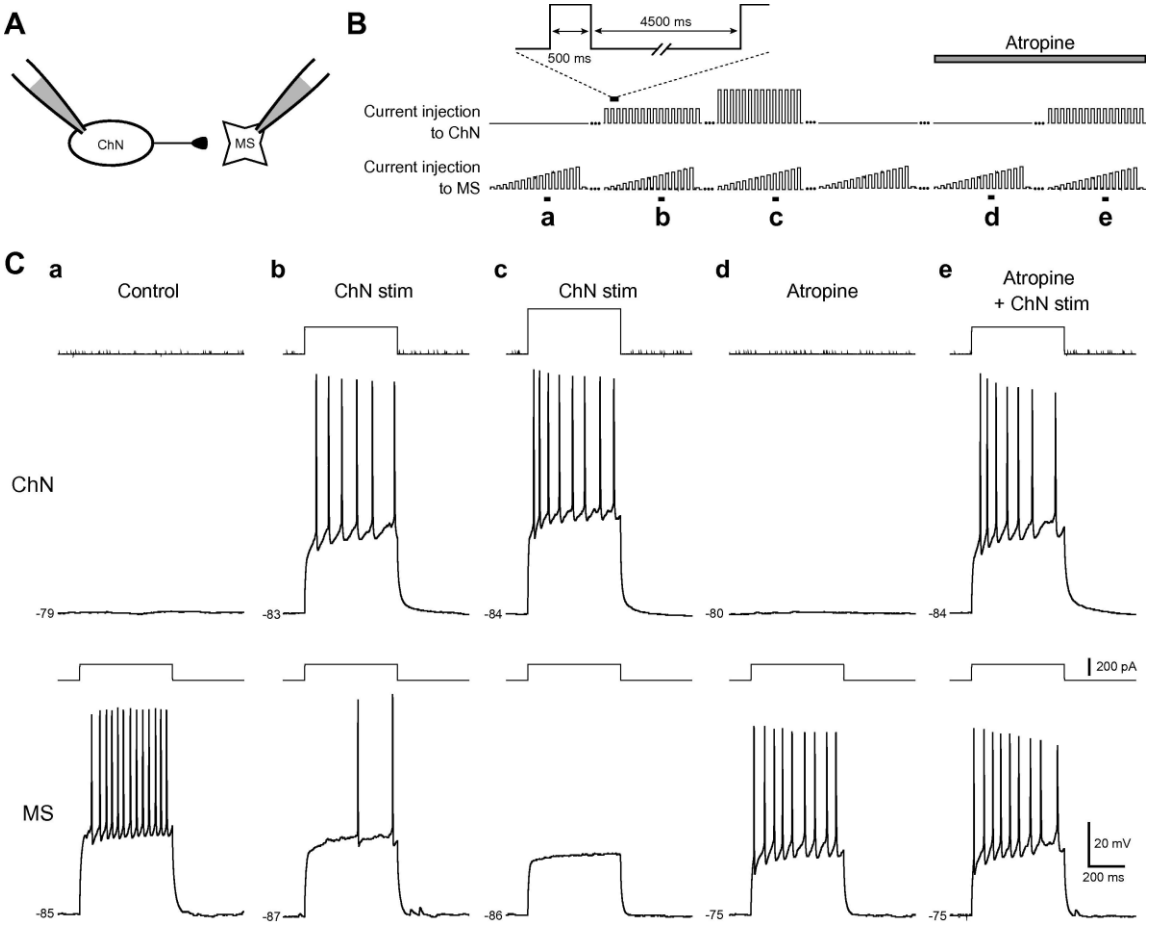

Figure 9. The suppressive effect of cholinergic neuronal activation on MS spike firing was blocked by atropine. ***A.*** Paired whole-cell patch clamp recording from an MS neuron and a cholinergic neuron. ***B.*** Repetitive depolarizing current pulses (15 pulses with Δ20 pA) were applied to the MS neuron (bottom trace). In the control, the cholinergic neuron was not stimulated (the early phase of recording). After the control recording, the constant depolarizing current pulses (inset) were injected in combination with stimulation of the MS neuron. ***C.*** Spike firing responses of the MS neuron without cholinergic spike firing during the period indicated by line ***a*** in panel ***B***. Cholinergic neuronal firing suppressed MS spike firing (***b, c***). Washout with application of atropine caused the MS spike firing to recover (***d***). Cholinergic stimulation in combination with atropine had little effect on MS spike firing (***e***).

Discussion

The present study examined cholinergic effects on the intrinsic electrophysiological properties MS neurons of the NAc by (1) bath application of carbachol and (2) electrical stimulation of a cholinergic interneuron adjacent to the MS neurons. It was found that carbachol depolarized the resting membrane potential with an increase in input resistance, which is in accordance with the results of previous studies in the striatum (Hsu et al., 1996). However, the slowly depolarizing potential, which regulates spike initiation, was suppressed by carbachol application and cholinergic neuronal stimulation.

Cholinergic action on the resting membrane potential and hyperpolarizing voltage responses

The present findings that carbachol depolarizes the resting membrane potential and increases input resistance in NAc MS neurons are consistent with those of previous studies in striatal MS neurons, in which M1 receptor-mediated reduction of potassium currents is demonstrated (Hsu et al., 1996, Hsu et al., 1997). The present results extend these findings by demonstrating a dose-dependent effect of carbachol on the resting membrane potential.

MS neurons exhibit inward rectification (Nisenbaum and Wilson, 1995), and the present study demonstrated the suppression of this rectification by carbachol (Fig. 6). It is known that inwardly rectifying potassium currents are involved in hyperpolarizing voltage responses in the striatum (Nisenbaum and Wilson, 1995). Uchimura et al. (1989) reported large contribution of inwardly rectifying potassium currents to the resting membrane potential of NAc MS neurons. Therefore, the activation of cholinergic, especially muscarinic, receptors is likely to inhibit inwardly rectifying potassium currents in this study (Galarraga et al., 1999).

Cholinergic effects on MS spike firing

In contrast to the increase in the voltage response to hyperpolarizing current injection, the present study demonstrated that carbachol reduced the slowly depolarizing potential responding to positive current injection, and in turn, decreased responsiveness. As a result, the rheobase was increased, even though the resting membrane potential was depolarized by carbachol. This cholinergic modulation is consistent with the report that acetylcholine decreases spike discharge by modulating A-currents (Akins et al., 1990). However, contradictory findings regarding the cholinergic modulation of spike firing have also been reported. In striatal MS neurons, cholinergic stimulation induces an increase in the spike firing rate (Galarraga et al., 1999, Zhang and Warren, 2002, Perez-Rosello et al., 2005). KCNQ currents, which regulate subthreshold membrane potentials and depolarize spike thresholds in striatal MS neurons, are also suppressed by a cholinergic agonist (Shen et al., 2005).

It is worth focusing on the differential modulatory patterns of acetylcholine on neural activities in MS neurons. The voltage dependency of the A-current may play a critical role in the contradictory effects of cholinergic agonists on MS neuronal firing. Akins et al. (1990) suggest that cholinergic agonists shift the activation and inactivation curves towards a negative potential as the peak conductance increases. Therefore, it seems rational to postulate that the resting membrane potential may influence on the dichotomous cholinergic effects on spike firing. Acetylcholine suppresses excitatory inputs at hyperpolarized membrane potentials, but it facilitates excitatory inputs at depolarized resting potentials (Akins et al., 1990). The deep resting membrane potential and a suitable protocol for the activation of the A-current (step pulses) with regard to ramp depolarization (Galarraga et al., 1999) may induce the cholinergic suppression of spike firing observed in this study.

Another possibility is that the MS neuronal sensitivity to acetylcholine varies. The activation of muscarinic receptors either suppressed or enhanced persistent potassium currents

in striatal MS neurons (Gabel and Nisenbaum, 1999). There might be a difference between the striatum and NAc with regard to the population of potassium currents. It is also possible that different cholinergic modulation depends on the expression of D_1- and D_2-like receptors. However, not a few NAc MS neurons express both D_1- and D_2-like receptors (Ridray et al., 1998), and the present results demonstrated no correlation between the cholinergic effects on the rheobase and electrophysiological properties including the resting membrane potential, input resistance, and rheobase, which may reflect the difference of MS neurons with D_1 and D_2 receptors (Gertler et al., 2008). Therefore, it was considered that different cholinergic modulation depending on the expression of D_1 and D_2 receptors is less likely.

Cholinergic interneuronal activation

Paired recordings from MS neurons and cholinergic interneurons have been performed to examine the effects of intrinsic acetylcholine on electrophysiological functions in the striatum (Lin et al., 2004, Shen et al., 2005, Pakhotin and Bracci, 2007). In agreement with this previous work, the spike induction in a cholinergic neuron is likely to induce acetylcholine release in the NAc. The activation of cholinergic interneurons exerted suppressive effects on the slowly depolarizing potential, which is in agreement with the results obtained with bath application of carbachol. However, the resting membrane potential was essentially unchanged by the stimulation of a cholinergic interneuron. In consideration of the dose dependency of carbachol on the resting membrane potential (Fig. 3C), the release of acetylcholine via the stimulation of a cholinergic interneuron is less than 1 μM. This is insufficient to depolarize the resting membrane potential. This finding supports the possibility that potassium channels that regulate the slowly depolarizing potential might have higher sensitivities to acetylcholine than inwardly rectifying potassium channels.

Direct effects of acetylcholine on MS neuronal activities

Dopamine is another critical neuromodulator that regulates the neural activities of NAc MS neurons; therefore, the suppressive cholinergic effects of NAc MS spike firing might be mediated by dopamine. Indeed, cholinergic activation increases dopamine release in the NAc (Kitamura et al., 1999). However, this possibility is unlikely because carbachol increased the rheobase under the presence of dopaminergic receptor blockers. Furthermore, several studies report that dopaminergic agonists increase the spike firing frequency of MS neurons in the NAc (Hopf et al., 2003, Chen et al., 2006), and subthreshold response, including those of the resting membrane potential and input resistance are not changed by dopamine (Hopf et al., 2003, Chen et al., 2006). These findings support the idea that acetylcholine directly regulates the electrophysiological properties of the NAc MS neurons and that this regulation is not mediated by dopamine release.

Acetylcholine elicits excitatory fast synaptic transmission via nicotinic receptors in several regions of the central nervous system. Although the present study showed 36 pairs of MS and cholinergic neurons, no excitatory postsynaptic transmission was observed. This is in line with the previous report that the striatal cholinergic interneurons induced EPSPs only in the NPY-NGF neurons (English et al., 2012). The present cholinergic effects were therefore likely to be mediated by a volume transmission mechanism (Contant et al., 1996).

Functional implications

In awake and unrestrained rats, the iontophoretic application of acetylcholine primarily suppresses MS neuronal activities in the NAc (Windels and Kiyatkin, 2003). This cholinergic suppression of MS neuronal activity is mediated by the postsynaptic muscarinic receptors in MS neurons and the presynaptic nicotinic receptors on dopaminergic terminals. Thus, the cholinergic suppression of MS neuronal firing observed in this study may elucidate a part of

the cellular mechanism by which spontaneous MS neuronal activity in the NAc is inhibited by the *in vivo* iontophoretic application of acetylcholine (Windels and Kiyatkin, 2003).

It is also possible that cholinergic modulation of neuronal firing might be attributable to the effects on excitatory and/or inhibitory synaptic transmission mediated by glutamatergic and GABAergic receptors, respectively. Several studies have reported an increase in the spontaneous firing rate caused by iontophoresis of acetylcholine in *in vivo* anesthetized preparations (Bernardi et al., 1976) and *in vitro* preparations (Takagi and Yamamoto, 1978). In accordance with the results of these studies, a suppressive effect of acetylcholine on IPSP amplitude is reported in the NAc (Sugita et al., 1991) and the caudate (Bernardi et al., 1976). However, EPSP amplitudes are also suppressed by acetylcholine via muscarinic receptors in the striatum (Dodt and Misgeld, 1986, Akaike et al., 1988, Calabresi et al., 1998). Thus, these effects of acetylcholine on MS spike firing initially appear contradictory, and they cannot be explained by a summation of the cholinergic effects on glutamatergic and GABAergic synaptic transmission. Thus, synaptic modulation by acetylcholine should be further analyzed in future work.

CHAPTER II

Reciprocal regulation of inhibitory synaptic transmission by nicotinic and muscarinic receptors in rat nucleus accumbens shell

Yamamoto K, Ebihara K, Koshikawa N, Kobayashi M. *J Physiol* 591: 5745-5763, 2013.

Introduction

The cholinergic system in the nucleus accumbens (NAc), a rostroventromedial extension of the striatum, plays critical roles in reward-related behaviors, drug abuse (Witten et al., 2010), and motor control (Kitamura et al., 1999). Medium spiny (MS) neurons are the principal neurons in the NAc, which project to the ventral pallidum and the midbrain dopaminergic cell areas, including the ventral tegmental area, the substantia nigra pars compacta, and the retrorubral field (Groenewegen et al., 1991). Although NAc cholinergic interneurons are considered to occupy only <2% of the neural population (Phelps et al., 1985; Rymar et al., 2004; Threlfell & Cragg, 2011), their axons are densely distributed in the NAc and project to the MS neurons (Zhou et al., 2003). A previous study using optogenetics demonstrated that the activation of NAc cholinergic interneurons suppresses the spontaneous firing of MS neurons in freely moving rats (Witten et al., 2010).

Glutamatergic inputs from the prefrontal cortex, medial thalamic nucleus, hippocampus, and basolateral amygdala drive MS neuronal activities (Groenewegen et al., 1991; Pennartz et al., 1994; Shinonaga et al., 1994). In contrast, MS neurons receive input from at least two GABAergic inhibitory neurons, e.g. the parvalbumin-immunopositive fast-spiking (FS) neurons and MS neurons themselves (Pennartz & Kitai, 1991; Kawaguchi et al., 1995; Taverna et al., 2004; Taverna et al., 2005, 2007; Kohnomi et al., 2012). Paired whole-cell patch-clamp recordings have revealed that FS neurons potently suppress postsynaptic MS neurons due to their high-frequency repetitive spike firing, the large amplitude of unitary inhibitory postsynaptic currents (uIPSCs), and the low failure rate of uIPSCs in FS→MS connections (Taverna et al., 2007; Kohnomi et al., 2012). In contrast, the recurrent collateral connections of MS neurons exhibit lower connection rate and smaller amplitude of uIPSCs in comparison to the FS neurons (Taverna et al., 2007; Kohnomi et al., 2012). These MS→MS connections are physiologically significant. For example, rodent models of Parkinson's disease show disruptions of MS→MS connections (Taverna et al., 2008).

Cholinergic modulation of IPSCs has been reported in the NAc and the striatum. Nicotinic agonists, which open cation channels, increase the frequency of spontaneous IPSCs (sIPSCs) in MS neurons without changing their amplitude (de Rover et al., 2005; Witten et al., 2010) or with an increase in the sIPSC amplitude (de Rover et al., 2002). However, the frequency and amplitude of miniature IPSCs (mIPSCs), which are recorded during the application of a voltage-gated sodium channel blocker, are not affected by nicotine (de Rover et al., 2002), suggesting that the nicotinic action of sIPSCs is likely to be induced by the activation of presynaptic GABAergic neurons. In contrast, muscarinic agonists decrease the frequency and amplitude of sIPSCs (Calabresi et al., 2000; de Rover et al., 2002; Musella et al., 2010), and in accordance with muscarinic suppression of sIPSCs, evoked IPSC amplitude is also suppressed by a muscarinic type I agonist (Calabresi et al., 2000; Perez-Rosello et al., 2005). Related to muscarinic receptor activation, a muscarinic agonist decreases the frequency of mIPSCs without changing their amplitude (Musella et al., 2010), suggesting the involvement of presynaptic mechanisms in the muscarinic suppression of IPSCs. In combination with the roles of nicotinic and muscarinic receptors in controlling IPSC properties, it is difficult to predict the effects of the simultaneous stimulation of these

receptors with acetylcholine or a nonspecific cholinergic agonist. Indeed, the activation of cholinergic interneurons induces an increase in sIPSC frequency (de Rover et al., 2006; Witten et al., 2010); however, a blockade of acetylcholine esterase decreases sIPSC frequency (Musella et al., 2010). This contradictory modulation by acetylcholine may be dependent on the presynaptic neuron subtypes, e.g., MS neurons and FS neurons. However, the relationship between the cholinergic modulation of IPSCs and the presynaptic cell subtypes has remained elusive in the NAc.

To comprehensively clarify the cholinergic regulation of inhibitory synaptic transmission in the NAc, it is necessary to discriminate the source of GABAergic inputs into the MS neurons. The present study performed paired whole-cell patch clamp recordings to distinguish the presynaptic neuron and postsynaptic neuron subtypes and examined the nicotinic and muscarinic effects on uIPSCs obtained from MS neurons in the NAc shell.

Methods

Unitary and miniature IPSC recordings

The techniques for slice preparation and whole-cell patch-clamp recording were similar to those described in Chapter I. Briefly, 63 vesicular GABA transporter (VGAT)-Venus line A transgenic rats (Uematsu et al., 2008) of either sex at 15 to 32 days old were used for recording. Whole-cell recording was performed using the pipette solution as follows (in mM): 70 potassium gluconate, 70 KCl, 10 *N*-(2-hydroxyethyl)piperazine-*N'*-2-ethanesulfonic acid (HEPES), 15 biocytin, 0.5 EGTA, 2 $MgCl_2$, 2 magnesium adenosine triphosphate (ATP), and 0.3 sodium guanosine triphosphate (GTP). In some of the uIPSC recordings, 10 mM 2-bis(2-aminophenoxy)ethane-*N,N,N',N'*-tetraacetic acid (BAPTA) was added to the above pipette solution to chelate intracellular Ca^{2+}. The pipette solution used for mIPSC recordings included the following components (in mM): 120 cesium gluconate, 20 biocytin, 10 HEPES, 8 NaCl, 5 *N*-(2,6-dimethylphenylcarbamoylmethyl) triethylammonium bromide (QX-314), 2 magnesium ATP, 0.3 sodium GTP and 0.1 BAPTA. Both pipette solutions had a pH of 7.3 and an osmolarity of 300 mOsm. The liquid junction potentials for uIPSC and mIPSC recordings were -9 mV and -12 mV, respectively, and the voltage was corrected accordingly.

Before uIPSC recordings, the voltage responses of presynaptic and postsynaptic cells were recorded by applying long hyperpolarizing and depolarizing current pulse (300 ms) injections to examine repetitive firing patterns. Several cell pairs had mutual or $\geq$ 2 connections; therefore, all cells were recorded under voltage-clamp conditions (holding potential = -80 mV) during uIPSC recordings. Short depolarizing voltage-step pulses (2 ms, 80 mV) were applied to presynaptic cells to induce action currents. Cholinergic agonists, such as carbachol, pilocarpine, nicotine, and acetylcholine, and antagonists, such as atropine, pirenzepine, and hexamethonium were added directly to the perfusate. uIPSCs were recorded in normal ACSF for 5-10 min; cholinergic agonists were applied for 7.5-12.5 min and then washed for 10 min. mIPSCs were recorded under the application of 1 μM tetrodotoxin, 50 μM D(-)-2-amino-5-phosphonopentanoic acid (D-APV), and 20 μM 6,7-dinitroquinoxaline-2,3-dione (DNQX). The cholinergic agonist application protocol during mIPSC recordings was similar to the protocol used for uIPSCs. Cholinergic antagonists or the type 1 cannabinoid receptors (CB_1) antagonist, *N*-(piperidin-1-yl)-5-(4-indophonyl)-1-(2,4-dichlorophenyl)-4-methyl-1H-pyrazole-3-carboxamide (AM251), were applied prior to the application of cholinergic agonists.

Data analysis

Clampfit (pClamp 10, Axon Instruments) was used to analyze voltage responses under the current clamp conditions and uIPSCs. Input resistance was measured from slopes of least-squares regression lines fitted to voltage-current (*V-I*) curves measured at the peak voltage deflection (current pulse amplitude up to -100 pA). The membrane time constant (τ_m) was obtained from a single exponential fit from baseline (the resting membrane potential) to the negative peak of a hyperpolarizing voltage response. The amplitude of the action potential was measured from the resting membrane potential. By application of depolarizing step current pulses (300-500 ms), repetitive firing was evaluated by slope of least-squares regression lines in a plot of the number of spikes versus the amplitude of injected current, i.e. frequency-current (*F-I*) curve (up to approximately 450 pA).

The amplitudes of the uIPSCs were measured as the difference between the peak postsynaptic currents and the baseline currents taken from a 2-3 ms time window close to the onset of the current. To measure the 20-80% rise time, 80-20% decay time, and decay time constants of uIPSCs, postsynaptic 10 events were aligned to the peak of presynaptic action currents and averaged. The decay phase of uIPSCs was not well fitted by a single exponential

function, and therefore, a double exponential function was used for fitting uIPSC decay curves as follows:

$$f(t) = A_{fast} \exp(-t/\tau_{fast}) + A_{slow} \exp(-t/\tau_{slow}) \quad (1)$$

where A_{fast} and A_{slow} are the amplitudes of fast and slow decay components, respectively, and τ_{fast} and τ_{slow} are their respective decay time constants. Weighted decay time constant (τ_w) was calculated using the following equation (Bacci et al., 2003):

$$\tau_w = [(A_{fast}\tau_{fast}) + (A_{slow}\tau_{slow})]/(A_{fast} + A_{slow}) \quad (2)$$

mIPSCs were detected at a threshold of 3-fold the standard deviation of the baseline noise amplitude using event detection software (kindly provided by Prof. John Huguenard, Stanford University). To measure the amplitude and interevent interval, mIPSCs were analyzed from continuous 5-7 min recordings just before and 5-7 min after the application of cholinergic agonists. To obtain cumulative plots of the interevent interval and the amplitude of mIPSCs, 100 events were summed per each MS neuron.

Data are presented as the mean ± standard error of the mean (SEM). Comparisons of the uIPSC amplitude and the paired-pulse ratio (PPR) between control and drug applications were conducted using the paired *t*-test. The distribution of the failure rate was not fitted using normal distribution; therefore, the nonparametric Wilcoxon test was applied for comparisons. Student's *t*-test was used for comparison of the percentage of cholinergic suppression of uIPSC amplitude. The amplitude and interevent interval of mIPSCs were analyzed using nonparametric statistical analysis (Kolmogorov-Smirnoff test; K-S test) to assess the significance of shifts in the cumulative probability distributions during the application of control compounds or cholinergic agonists. The paired *t*-test was used to compare the mean mIPSC amplitude and interevent intervals. $P < 0.05$ was considered to indicate significance.

Histology

To visualize recorded neurons after whole-cell patch-clamp recording, the slices were fixed, stored, and processed using a whole-mount protocol (Kobayashi et al., 2012). The slices were rinsed in 0.5% Triton X-100 and 0.1 M glycine in 0.1 M PB and then incubated with the Alexa 594 streptavidin fluorophore (5 mg/μL, Molecular Probes, Eugene, OR) in blocking solution overnight. The slices were rinsed in 0.5% Triton X-100 and 0.1 M glycine in 0.1 M PB, mounted on slides, and covered with Vectashield (Vector Laboratories). The slices were examined, and images were obtained with a confocal microscope (FV-1000, Olympus). Occasionally, the pipette solution used for uIPSC recordings (see above) in combination with Alexa Fluor 568 (1%, Molecular Probes) was used to visualize recorded MS neurons during electrophysiological recordings. All chemicals, unless otherwise specified, were purchased from Sigma-Aldrich (St. Louis, MO, USA).

Results

Figure 10 shows an example of dual recordings from two MS neurons. GABAergic neurons, including MS neurons, were identified by VGAT visualization using the VGAT-Venus line A transgenic rats (Fig. 10A). MS neurons exhibited abundant spines in their dendrites (Fig. 10B, C), and these findings indicate that the recorded neurons are MS neurons. In addition to the anatomical approaches used, MS neurons were identified by the following electrophysiological properties of neurons: (1) deep resting membrane potential, (2) high input resistance, and (3) ramp potential in response to depolarizing current pulses (Fig. 11A). In contrast, FS neurons showed high repetitive firing frequencies as previously reported (Taverna et al., 2007; Kohnomi et al., 2012; Table 2). According to the previous criteria (Kohnomi et al., 2012), the recorded neurons were divided into MS neurons and FS neurons. This study excluded cholinergic interneurons and persistent and low-threshold spike neurons (Kawaguchi et al., 1995).

In the first series of experiments, paired whole-cell patch-clamp recording was performed using NAc MS neurons to record uIPSCs, and investigated which types of cholinergic receptors are involved in the cholinergic modulation of uIPSCs. Second, the cholinergic modulation of FS→MS connections in the NAc was examined. The properties of uIPSCs in MS→MS and FS→MS connections are summarized in Table 3. Finally, mIPSCs were recorded from MS neurons to compare the findings obtained from uIPSC recordings.

Table 2. Intrinsic electrophysiological properties of NAc neurons

	Medium spiny neuron		Fast-spiking neuron	
	Mean ± S.E.M.	n	Mean ± S.E.M.	n
Vm [a] (mV)	-80.7 ± 0.5	100	-79.1 ± 1.1	20
Input resistance (MΩ)	268.0 ± 8.7	100	197.4± 19.0 **	20
τ_m [b] (ms)	5.4 ± 0.4	64	6.9 ± 0.3 *	9
Action potential				
Amplitude (mV)	98.9 ± 0.1	100	81.6 ± 2.4 ***	20
Half duration (ms)	1.91 ± 0.05	100	0.90 ± 0.06 ***	20
Repetitive spike firing				
F-I slope (Hz/pA)	0.25 ± 0.01	100	0.57 ± 0.04 ***	20

[a] Resting membrane potential; [b] membrane time constant. * $P < 0.05$, ** $P < 0.01$, *** $P < 0.001$, Student's *t*-test.

Table 3. Properties of uIPSCs from MS→MS and FS→MS connections

	MS→MS		FS→MS	
	Mean ± S.E.M.	n	Mean ± S.E.M.	n
Amplitude (pA)	40.0 ± 6.6	78	75.8 ± 19.8 *	21
20-80% rise time (ms)	1.3 ± 0.2	74	0.8 ± 0.1	21
80-20% decay time (ms)	19.1 ± 0.8	67	21.8 ± 1.6	21
τ_w [a] (ms)	16.4 ± 0.9	67	18.8 ± 2.3	21
Failure rate (%)	30.9 ± 3.0	79	16.7 ± 4.1 **	21

[a] Weighted decay time constant. * $P < 0.05$, ** $P < 0.01$, Student's *t*-test.

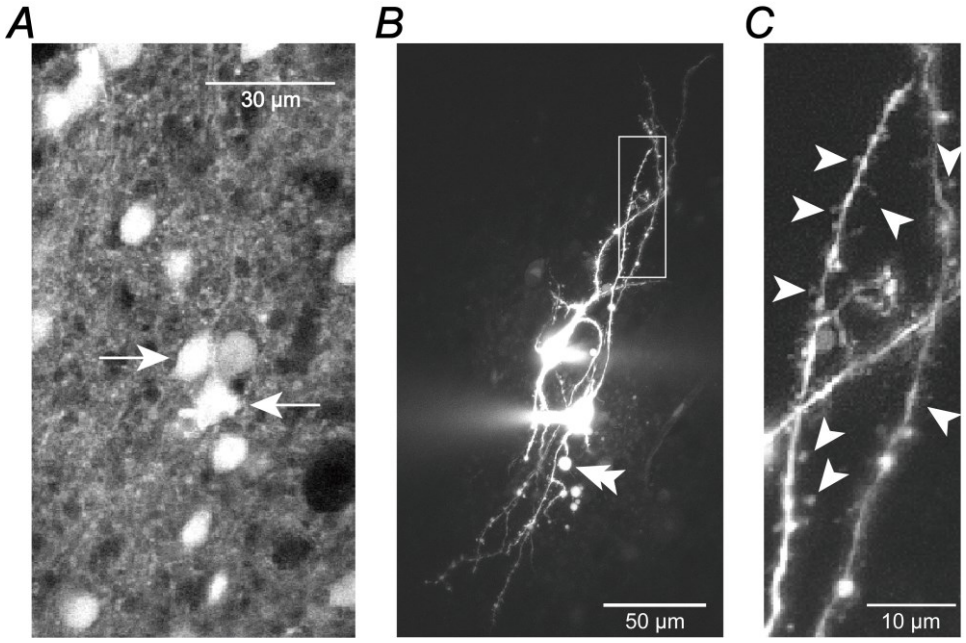

Figure 10. Morphological features of MS neurons in the NAc shell. **A**: An example of a fluorescence image of Venus-positive neurons. Paired whole-cell patch-clamp recording was performed from Venus-positive neurons as indicated by the arrows. **B**: The recorded neurons stained with a fluorescent dye (Alexa 568). The axon terminal bleb is indicated by a double arrowhead. **C**: Expanded images of the dendrites of the recorded neurons shown in **B**. Note the abundant spines (arrowheads), which indicate that the recorded neurons are MS neurons.

Suppression of uIPSCs in MSN→MSN connections by carbachol

To explore the temporal properties of the modification of uIPSCs by the nonselective cholinergic agonist carbachol, paired-pulse stimuli were applied to presynaptic MS neurons at 20 Hz. A typical example of a paired whole-cell patch-clamp recording from two MS neurons is shown in Fig. 11. The slowly depolarizing ramp potential, which is a characteristic property of MS neurons (Kawaguchi et al., 1995; Kohnomi et al., 2012), was induced in response to a long depolarizing current pulse just above the rheobase (Fig. 11A).

The action current induction by short depolarizing voltage pulse injections (1 ms, 80 mV) into the presynaptic MS neuron (MS1) elicited uIPSCs in the postsynaptic MS neuron (MS2). The bath application of 1-10 µM carbachol suppressed the amplitude of the first uIPSC, which was recovered after 10 min of washing (Fig. 11B, D). The rise and decay kinetics of uIPSCs were comparable, as shown by the scaled uIPSCs (Fig. 11C). The scaled uIPSCs also indicated that carbachol-induced suppression was more prominent in the 1st uIPSC compared to the 2nd uIPSC; i.e., PPR was increased by carbachol.

In 33 MS→MS connections, the application of 1 µM carbachol suppressed the amplitude of the 1st uIPSC by 58.3 ± 8.0% (34.8 ± 7.3 pA to 15.2 ± 4.3 pA; $P < 0.001$, paired *t*-test, Fig. 11G). The carbachol-induced suppression of the uIPSC amplitude was accompanied by an increase in the PPR from 0.65 ± 0.05 to 1.30 ± 0.17 ($P < 0.001$, paired *t*-test) and the failure rate of the 1st uIPSC from 30.3 ± 4.7% to 63.5 ± 5.1% ($P < 0.001$, Wilcoxon test). These results suggest that carbachol suppresses the uIPSC amplitude via a presynaptic mechanism (Stevens & Wang, 1995; Jiang et al., 2000).

Atropine blocks carbachol-induced suppression of uIPSCs in MS→MS connections

The cholinergic receptors are divided into two classes: (1) the nicotinic receptors, which couple to ionic channels; and (2) the muscarinic receptors, which activate an intracellular cascade via G-proteins. To examine which receptor subtypes are involved in carbachol-

induced uIPSC suppression, the present study examined the effect of carbachol on uIPSCs under the application of atropine, a nonselective muscarinic antagonist.

An example of the effect of carbachol (10 μM) in combination with 100 μM atropine is shown in Fig. 11E, F. Under pre-application of atropine, carbachol had little effect on the uIPSC amplitude in the MS→MS connection. In 19 MS→MS connections, carbachol in combination with atropine did not significantly change the 1st uIPSC amplitude (96.5% of control; 42.4 ± 10.6 pA to 40.8 ± 12.1 pA; $P > 0.7$, paired t-test). In parallel to the insignificant effect on the uIPSC amplitude, carbachol with atropine did not change the PPR (0.68 ± 0.08 under atropine to 0.75 ± 0.08 with carbachol, n = 19; $P > 0.1$, paired t-test) or the failure rate (30.2 ± 6.3% under atropine to 38.2 ± 6.9% with carbachol, n = 19; $P > 0.6$, Wilcoxon test), as shown in Fig. 11H. Therefore, it is likely that carbachol suppresses the uIPSC amplitude via muscarinic receptors.

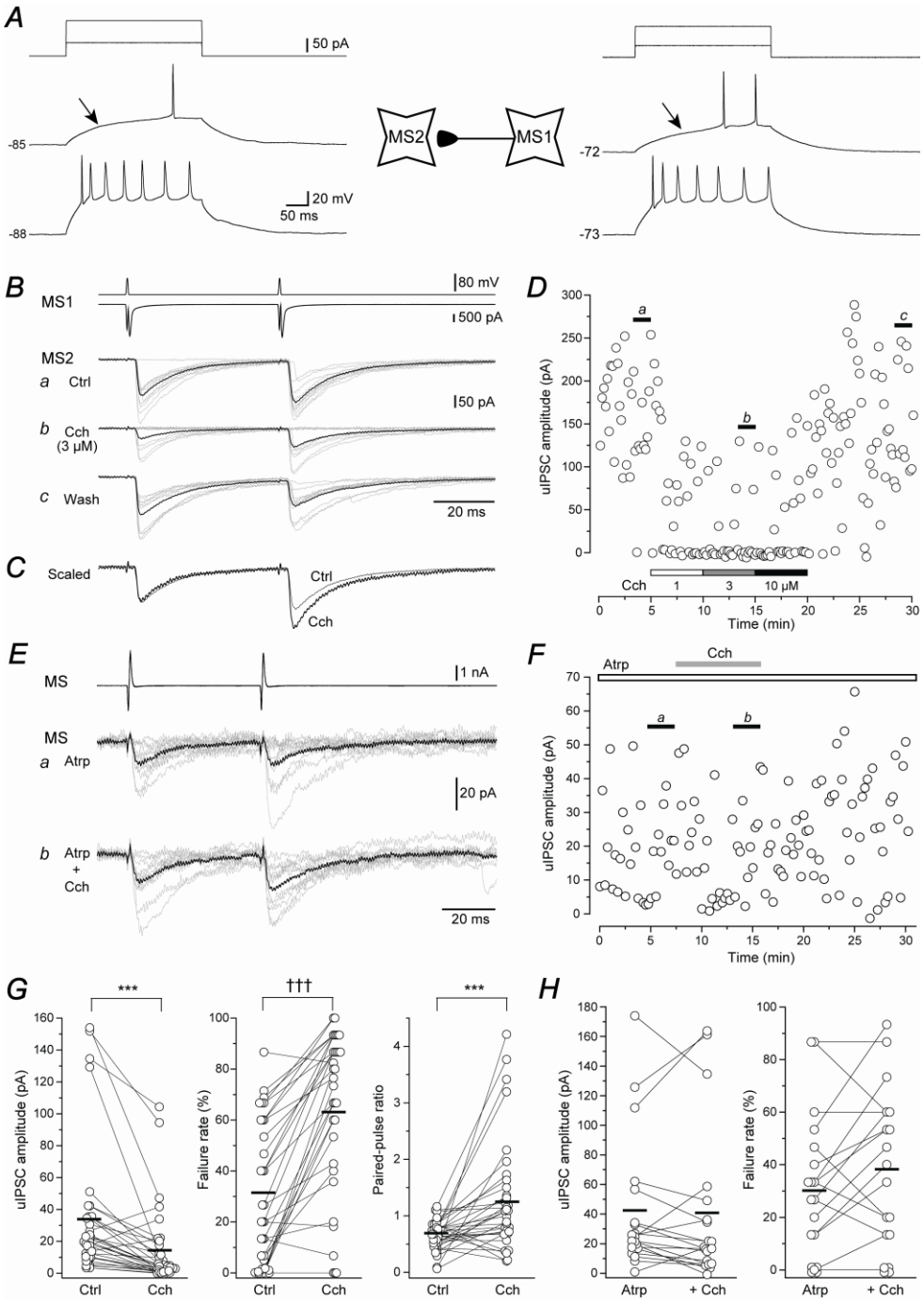

Figure 11. The effects of carbachol on unitary inhibitory postsynaptic currents (uIPSCs) recorded from MS→MS connections. **A**: A scheme of an MS→MS connection (MS1→MS2) with suprathreshold voltage responses of each MS neuron. The ramp depolarizing potential and temporal lags before spike firing are denoted by arrows. The resting membrane potentials are shown to the left of the traces. **B**: The effect of carbachol (Cch; 3 μM) on uIPSCs obtained from the MS1→MS2 connection in **A**. Action currents (second top traces) were induced by a depolarizing voltage step pulse injection to the presynaptic MS neuron (MS1). Responding to the action currents in the MS1, uIPSCs were observed in the postsynaptic MS neuron (MS2). Postsynaptic traces in control (Ctrl, ***a***), during carbachol application (***b***), and after washing (***c***) are shown. Ten consecutive traces are shown in grey lines, and averaged traces are shown in black. Note that carbachol suppresses uIPSC amplitude. **C**: The scaled uIPSCs in the control and during the carbachol application shown in **B**. Note the lesser effect of carbachol on the 2nd uIPSC. **D**: The time course of the uIPSC amplitude before, during and after carbachol (1, 3, and 10 μM) application in the MS1→MS2 connection shown in **A**-**C**. Short bars (**a**, **b**, and **c**) indicate the periods when the averaged traces in **B** were obtained. **E**: Typical traces under the application of 100 μM atropine alone (Atrp, **a**) and the co-application with 1 μM carbachol (Cch, **b**). Top traces show presynaptic action currents. Atropine blocks carbachol-induced suppression of uIPSCs in MS→MS connections. **F**: The time course of uIPSC amplitude on the application of atropine and carbachol shown in **E**. **G**: Carbachol-induced (1 μM) effects on the uIPSC amplitude, the failure rate, and the paired-pulse ratio in MS→MS connections (n = 33). **H**: A summary of the uIPSC amplitude and the failure rate under the application of atropine alone and the co-application with carbachol. No significant difference between these two groups was observed (n = 19). *** $P < 0.001$, paired *t*-test. ††† $P < 0.001$, Wilcoxon test.

Pilocarpine mimics carbachol-induced suppression of uIPSCs in MS→MS connections

In addition to the experiment using the muscarinic antagonist, the effect of the nonselective muscarinic agonist pilocarpine was examined in MS→MS connections. A typical example of the effect of pilocarpine on uIPSCs is shown in Fig. 12A, B. Bath application of 1 μM pilocarpine suppressed the 1st uIPSC amplitude; however, the 2nd uIPSC amplitude was less attenuated (Fig. 12A). The pilocarpine-induced suppression of uIPSCs in MS→MS connections was reversible (Fig. 12A, B). In 14 MS→MS connections, pilocarpine (1 μM) suppressed the 1st uIPSC amplitude from 24.1 ± 7.9 pA to 18.8 ± 7.4 pA ($P < 0.05$, paired *t*-test), which accompanied increases in the failure rate (41.2 ± 6.0% to 59.5 ± 8.0%; $P < 0.01$, Wilcoxon test) and in the PPR (0.61 ± 0.09 to 1.16 ± 0.22, $P < 0.05$, paired *t*-test; Fig. 12E). The suppression rates of uIPSCs were not different between carbachol (41.7 ± 8.0%, n = 33) and pilocarpine (59.3 ± 8.7%, n = 14; $P > 0.21$, Student's *t*-test). The holding current was not changed by 1 μM pilocarpine (-4.3 ± 2.2 pA, n = 15; $P > 0.08$, paired *t*-test).

Several studies have reported the involvement of M_1 receptors in the cholinergic modulation of IPSCs in MS neurons (Perez-Rosello et al., 2005; Musella et al., 2010), and the present muscarinic suppression of uIPSCs in MS→MS connections may be mediated by M_1 receptors. To examine this possibility, pilocarpine was applied in combination with pirenzepine (10 μM), an M_1 receptor antagonist (Fig. 12C, D). Under the application of pirenzepine, pilocarpine had little effect on uIPSC amplitude (41.8 ± 10.5 pA to 39.2 ± 9.5 pA, n = 12, $P > 0.28$, paired *t*-test) and the failure rate in MS→MS connections (36.4 ± 8.1% to 31.5 ± 8.1%, n = 12, $P > 0.18$, paired *t*-test; Fig. 12F), supporting the above hypothesis.

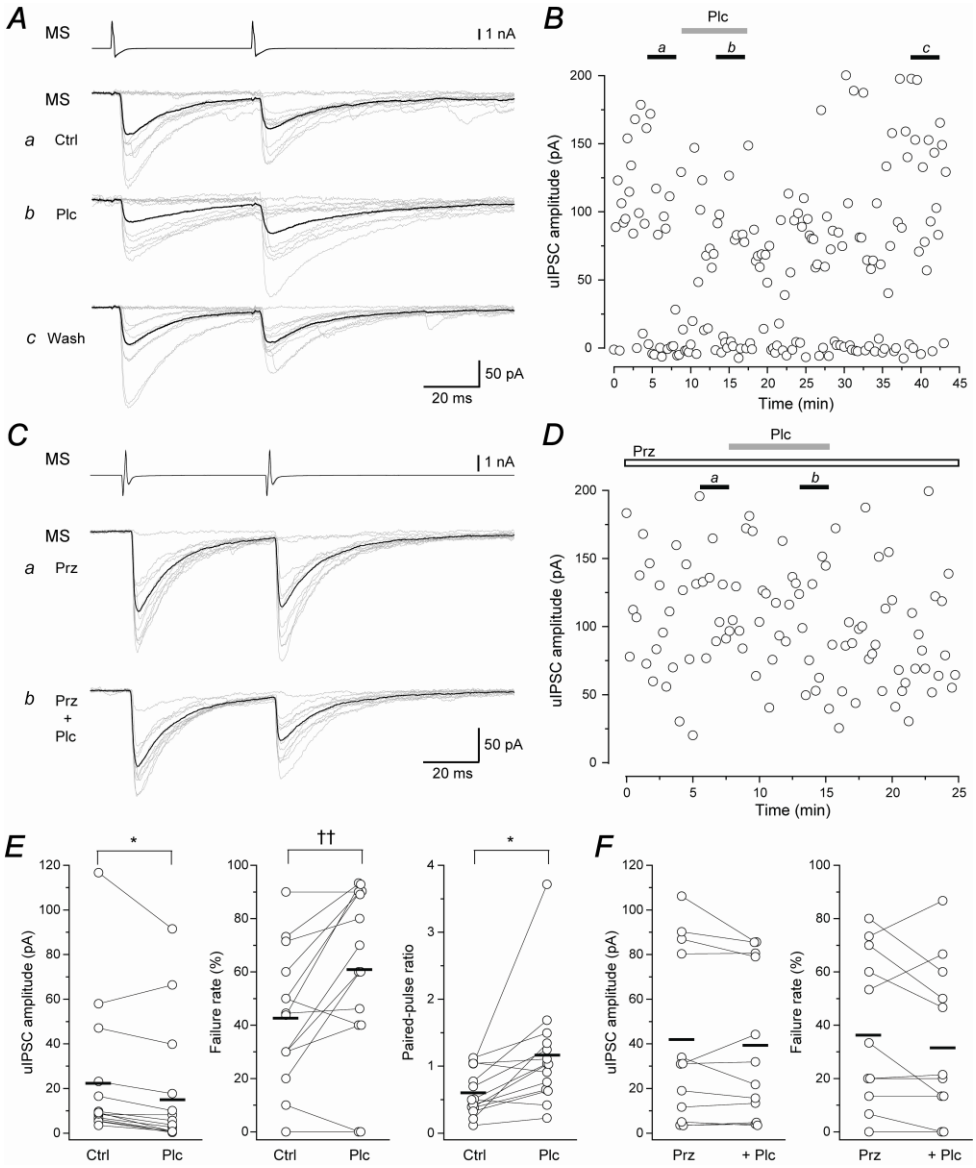

Figure 12. The application of pilocarpine (1 μM) mimics carbachol-induced uIPSC suppression in MS→MS connections. **A**: The suppressive effect of pilocarpine (Plc) on uIPSCs. Top traces show presynaptic action currents. **B**: The time course of uIPSCs before, during and after the pilocarpine application shown in **A**. **C**: Typical traces under the application of 10 μM pirenzepine alone (Prz, **a**) and the co-application with 1 μM pilocarpine (Plc, **b**). Pirenzepine blocks pilocarpine-induced suppression of uIPSCs in MS→MS connections. **D**: The time course of the uIPSC amplitude on the application of pirenzepine and pilocarpine shown in **C**. **E**: A summary of pilocarpine-induced effects on the uIPSC amplitude, the failure rate, and the paired-pulse ratio in MS→MS connections (n = 14). **F**: A summary of the uIPSC amplitude and the failure rate under the application of pirenzepine alone and co-application with pilocarpine. No significant difference between these two groups was observed (n = 12). * $P < 0.05$, paired *t*-test. †† $P < 0.01$, Wilcoxon test.

Nicotine had little effect on uIPSCs in MS→MS connections

Several studies have demonstrated the contribution of nicotinic receptors to excitatory synaptic transmission in the striatum and the NAc (English et al., 2012); however, no information is currently available regarding nicotinic modulation of IPSCs in the NAc. Although the experiments using the muscarinic agonist and antagonist described above suggest that nicotinic modulation of uIPSCs in the NAc is not very likely, the effect of nicotine was examined to obtain direct evidence of less contribution of nicotinic receptors to uIPSCs. Fig. 13A and B show a typical example of the nicotinic effect on uIPSCs in the

MS→MS connection. Bath application of 1 μM nicotine had little effect on the amplitude of uIPSCs. In 11 connections between MS neurons, nicotine did not change the uIPSC amplitude (22.9 ± 5.6 pA to 17.7 ± 4.5 pA, $P > 0.11$, paired *t*-test) or the failure rate (38.3 ± 8.7% to 39.1 ± 6.7%; $P > 0.14$, Wilcoxon test). The holding current was not changed by 1 μM nicotine (0.4 ± 4.7 pA, n = 11; $P > 0.93$, paired *t*-test).

These results support the hypothesis that the carbachol-induced suppression of uIPSCs in MS→MS connections is mediated by presynaptic muscarinic receptors.

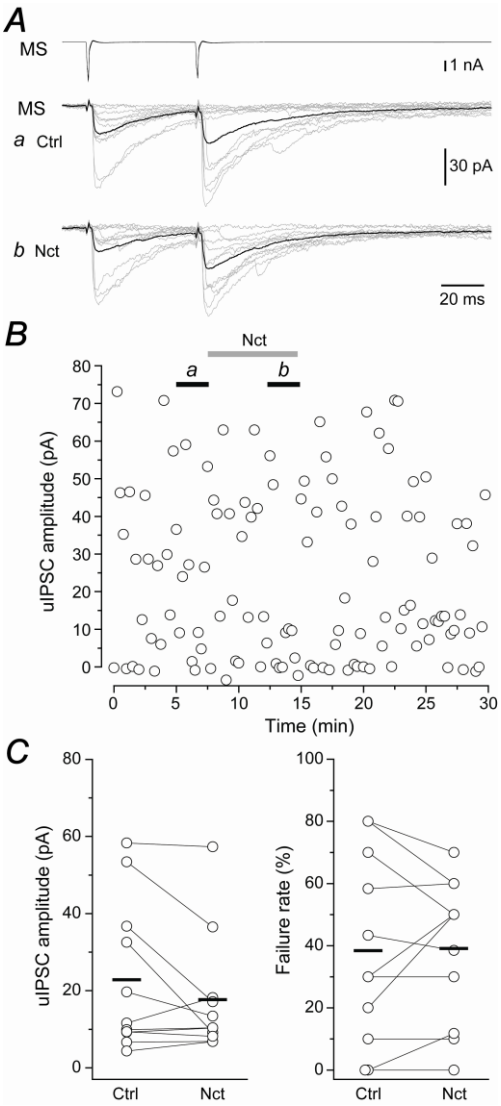

Figure 13. Effects of nicotine (1 μM) on uIPSCs in MS→MS connections. **A**: Little effect of nicotine on uIPSCs. The top traces show presynaptic action currents, and the middle and the bottom traces show uIPSCs in the control (Ctrl, **a**) and under the application of nicotine, respectively (Nct, **b**). **B**: The time course of the uIPSCs before, during and after the nicotine application shown in **A**. **C**: A summary of the uIPSC amplitude and the failure rate under the application of nicotine in comparison to the control. No significant difference between these two groups was observed (n = 11).

Effects of endocannabinoid signaling on muscarinic uIPSC modulation in MS→MS connections

Narushima et al. (2007) have reported that the muscarinic suppression of evoked IPSCs requires postsynaptic endocannabinoid signaling in the striatum, suggesting the possibility that the present muscarinic suppression of uIPSCs in MS→MS connections could be

mediated by endocannabinoid. To test this possibility, the effects of carbachol or pilocarpine were examined under the application of 5 μM AM251, a CB_1 receptor antagonist, on uIPSCs in MS→MS connections. In addition, the cholinergic suppression of uIPSCs was examined in combination with intracellular injection of 10 mM BAPTA, a Ca^{2+} chelator, into the postsynaptic MS neurons (see Methods).

Under the application of AM251, carbachol suppressed the 1st uIPSC amplitude by 30.8 ± 8.9% (30.7 ± 8.2 pA to 19.8 ± 5.3 pA, n = 16; $P < 0.01$, paired *t*-test; Fig. 14A, B, F), which was significantly smaller than that of carbachol (58.3 ± 8.0%; $P < 0.05$, Student's *t*-test). An example of the carbachol-induced suppression of uIPSCs in combination with BAPTA injection to postsynaptic MS neurons was shown in Fig. 14C-E. The recordings were started 20-25 min after the membrane rupture. The triple whole-cell patch-clamp recording shows that the postsynaptic MS neuron with 10 mM BAPTA (MS2) exhibited a similar carbachol-induced suppression of uIPSC amplitude in comparison to the postsynaptic MS neuron without BAPTA (MS3). The average rate of carbachol-induced suppression of uIPSCs with BAPTA was 46.3 ± 21.6% (63.3± 11.5 pA to 28.0 ± 8.3 pA, n = 5; $P < 0.05$, paired *t*-test), which was not significantly different from that without BAPTA (58.3 ± 8.0%; $P < 0.05$, Student's *t*-test; Fig. 14F). Pilocarpine (1 μM) with AM251 suppressed the 1st uIPSC amplitude by 26.6 ± 11.0% (30.9 ± 5.5 pA to 23.6 ± 5.4 pA, n = 6; $P < 0.05$, paired *t*-test), which was not significantly different from that of pilocarpine (40.7 ± 8.7%; $P > 0.38$, Student's *t*-test; Fig. 14F).

These results suggest that endocannabinoid signaling contributes the muscarinic suppression of uIPSCs in the NAc MS→MS connections in part but not in whole.

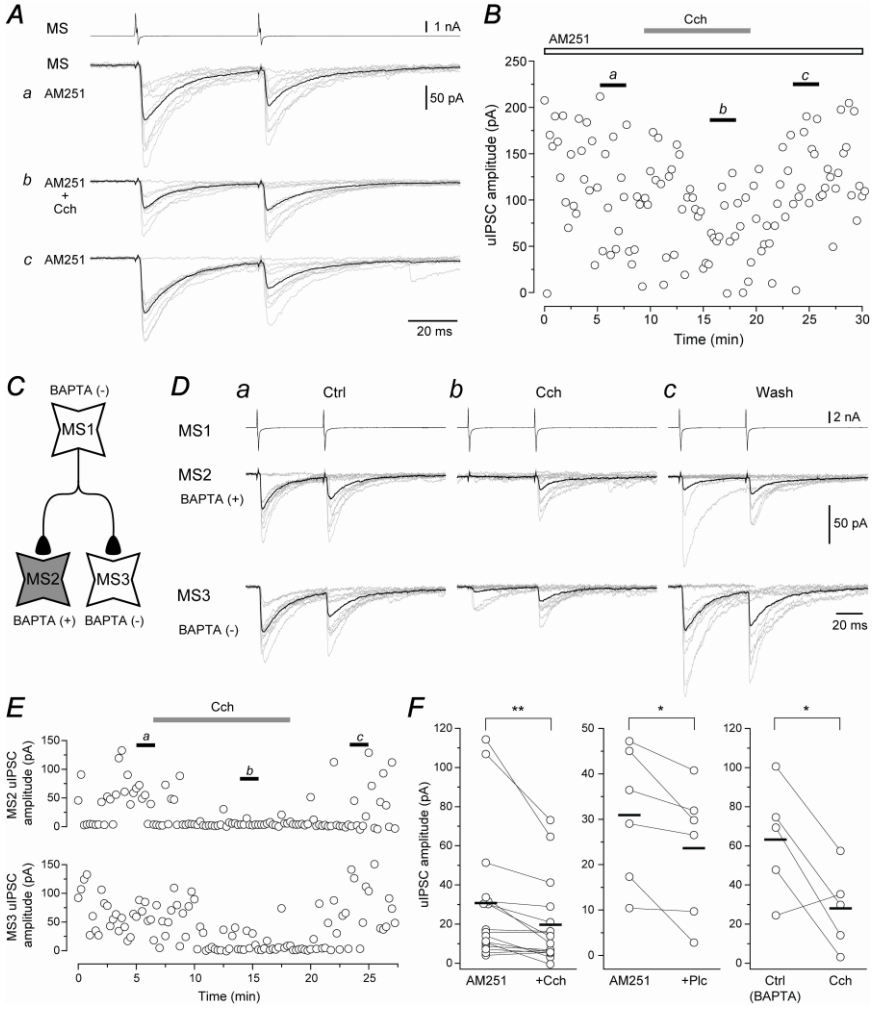

Figure 14. Effects of endocannabinoid signaling on carbachol- or pilocarpine-induced suppression of uIPSCs in MS→MS connections. **A**: Typical traces under the application of 5 μM AM251 alone (AM251, **a**), during the co-application with 1 μM carbachol (Cch, **b**), and after washing (**c**). Top traces show presynaptic action currents. Carbachol suppressed uIPSCs under application of AM251. **B**: The time course of uIPSC amplitude on the application of AM251 and carbachol shown in **A**. **C**: A scheme of triple whole-cell patch-clamp recordings from MS neurons. BAPTA (10 mM) was injected in MS2 neuron. **D**: Both MS2 and MS3 showed the carbachol (1 μM)-induced uIPSC suppression. **E**: The time courses of uIPSC amplitude shown in **D**. **F**: A summary of the uIPSC suppression by 1 μM carbachol with 5 μM AM251 (*left*, n = 16), 1 μM pilocarpine (Plc) with AM251 (*middle*, n = 6), and carbachol in combination with postsynaptic injection of 10 mM BAPTA (*right*, n = 5). * $P < 0.05$, paired *t*-test. ** $P < 0.01$, paired *t*-test.

Nicotine but not pilocarpine facilitates uIPSCs in FS→MS connections

FS neurons are another source of GABAergic inputs into MS neurons. Although the population of FS neurons in the NAc shell is less than 5%, the uIPSC amplitude in FS→MS connections is larger than the amplitude observed in MS→MS connections (Taverna et al., 2007; Kohnomi et al., 2012), suggesting that FS neurons provide pivotal inhibitory inputs to MS neurons in the NAc. In the following experiments, we examined the cholinergic effects on FS→MS connections.

In contrast to MS→MS connections, which showed little change in the uIPSC amplitude by nicotine, FS→MS connections showed the nicotine-induced facilitation of uIPSCs (Fig. 15A-D, G). Bath application of 1 μM nicotine increased the uIPSC amplitude from 44.6 ± 11.6 pA to 54.6 ± 12.7 pA (n = 11; $P < 0.01$, paired *t*-test). The nicotine-induced facilitation of uIPSCs was accompanied by a decrease in the failure rate (25.0 ± 6.8% to 15.0 ± 5.5%, n = 11; $P < 0.05$, Wilcoxon test) and the PPR (0.79 ± 0.08 to 0.61 ± 0.03, n = 11; $P < 0.05$, paired *t*-test), suggesting that nicotine facilitates GABA release from the FS presynaptic terminals. Preapplication of 5 μM hexamethonium, a nicotinic receptor antagonist, blocked the nicotine-induced uIPSC facilitation in FS→MS connections (59.0 ± 19.2 pA to 61.0 ± 19.0 pA, n = 6; $P > 0.31$, paired *t*-test; Fig. 15E, F, H). The failure rate was also not changed by nicotine under application of hexamethonium (19.7 ± 9.5% to 24.0 ± 11.5%, n = 6, $P > 0.46$, Wilcoxon test). The holding current was not changed by 1 μM nicotine (-4.9 ± 4.7 pA, n = 6; $P > 0.38$, paired *t*-test).

On the other hand, pilocarpine (1 μM) had little effect on the amplitude of uIPSCs in FS→MS connections (37.0 ± 10.7 pA to 35.9 ± 10.8 pA, n = 10; $P > 0.37$, paired *t*-test; Fig. 16). Similar to the insignificant effect of pilocarpine on the uIPSC amplitude, the failure rate was also less affected by pilocarpine (30.9 ± 9.3% to 29.8 ± 9.9%, n = 10; $P > 0.60$, Wilcoxon test). The holding current was not changed by 1 μM pilocarpine (12.6 ± 11.5 pA, n = 5; $P > 0.38$, paired *t*-test).

These results suggest that activation of nicotinic receptors facilitates uIPSC amplitude possibly via presynaptic mechanisms in FS→MS connections.

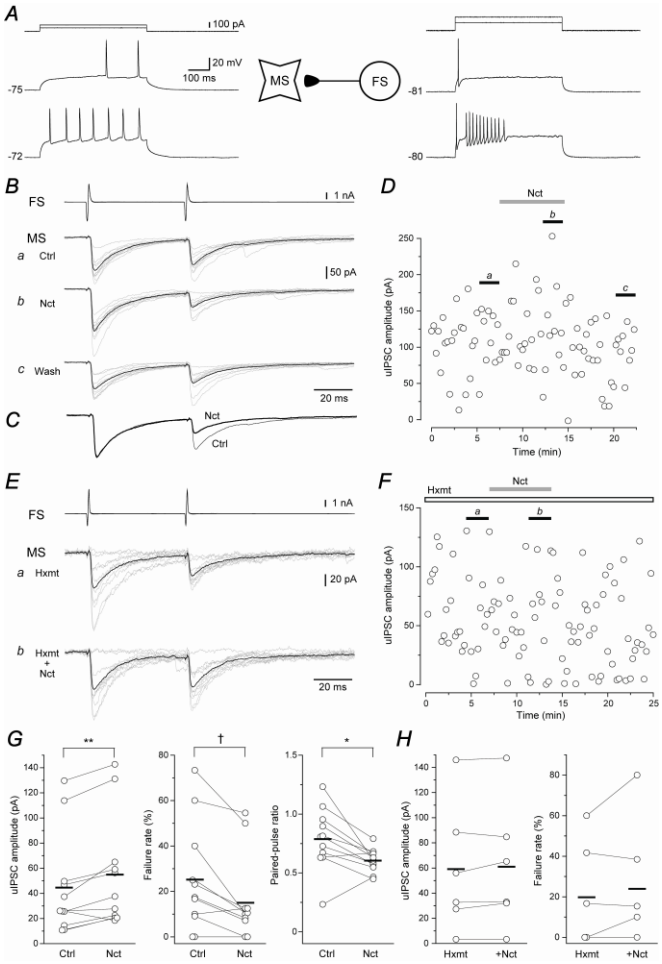

Figure 15. The effects of nicotine on uIPSCs recorded from fast-spiking (FS) →MS connections. **A**: A scheme of the FS→MS connection (FS→MS) with suprathreshold voltage responses. Deep afterhyperpolarization with a short duration and a high frequency of repetitive firing in FS neuron. **B**: The effect of 1 μM nicotine on uIPSCs in the FS→MS connection shown in **A**. Top traces show presynaptic action currents, and postsynaptic uIPSC traces are shown in the lower panels: **a**, control (Ctrl); **b**, during the application of nicotine (Nct), and **c**, after the wash. Ten consecutive traces are shown in grey lines, and averaged traces are shown in black. Note that nicotine increases the uIPSC amplitude. **C**: The scaled uIPSCs in the control and during the nicotine application shown in **B**. Note the decrease in the paired-pulse ratio caused by nicotine. **D**: The time course of the uIPSC amplitude before, during and after nicotine application in the FS→MS connection shown in **A**-**C**. **E**: Under the application of 5 μM hexamethonium (Hxmt), a nicotinic receptor antagonist, nicotine (1 μM) had little effect on the uIPSC amplitude in the FS→MS connection. **F**: The time course of the uIPSC amplitude before, during and after nicotine application with hexamethonium shown in **E.** **G**: Nicotine-induced effects on the uIPSC amplitude, the failure rate, and the paired-pulse ratio in FS→MS connections (n = 11). **H**: A summary of the effect of 1 μM nicotine with 5 μM hexamethonium on uIPSCs (n = 6). * $P < 0.05$, paired *t*-test; ** $P < 0.01$, paired *t*-test. † $P < 0.05$, Wilcoxon test.

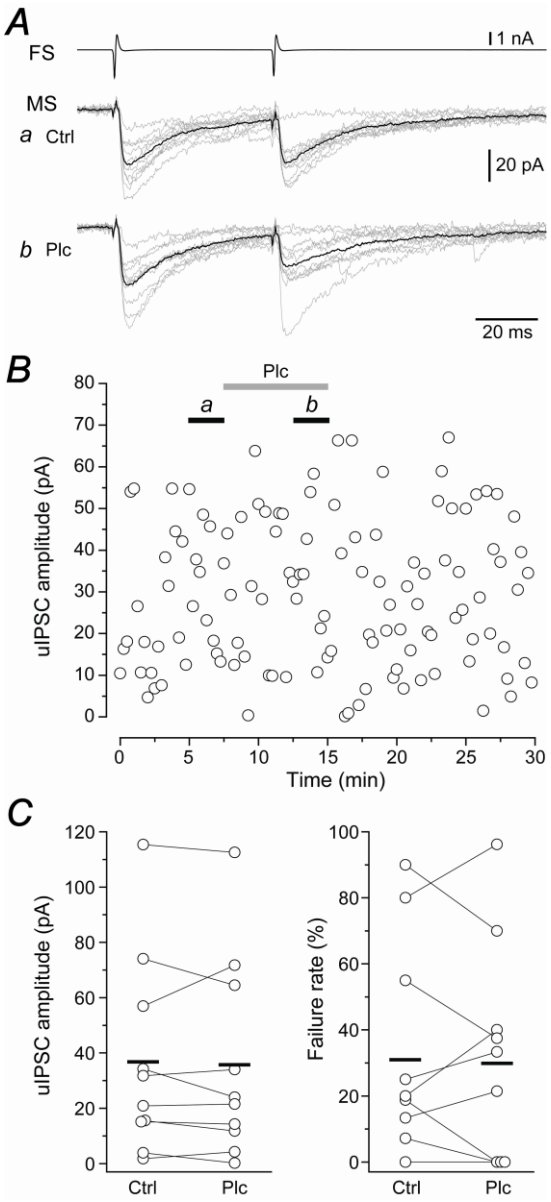

Figure 16. Effects of pilocarpine (1 μM) on uIPSCs in FS→MS connections. **A**: Little effect of nicotine on uIPSCs. Top traces show presynaptic action currents, and middle and bottom traces show uIPSCs in the control (Ctrl, **a**) and under the application of pilocarpine (Plc, **b**), respectively. **B**: Time course of uIPSCs before, during and after the pilocarpine application shown in **A**. **C**: A summary of the uIPSC amplitude and the failure rate under the application of pilocarpine in comparison to the control. No significant difference was observed between these two groups (n = 10).

Acetylcholine mimics carbachol-induced modulation of uIPSCs in MS→MS and FS→MS connections

To examine whether the cholinergic modulations of uIPSCs described above are mimicked by the endogenous ligand, acetylcholine, the effects of 1 μM acetylcholine on uIPSCs in MS→MS and FS→MS connections were examined.

In MS→MS connections, acetylcholine decreased the amplitude of uIPSCs from 26.5 ± 5.6 pA to 20.3 ± 4.7 pA (n = 9, $P < 0.01$, paired *t*-test), which was accompanied by increases in the failure rate (34.3 ± 6.7% to 48.6 ± 6.2%, n = 9; $P < 0.05$, Wilcoxon test) and the PPR (0.66 ± 0.08 to 1.06 ± 0.19, n = 9; $P < 0.05$, paired *t*-test; Fig. 17A-C, G). On the other hand, the FS→MS connection in Fig. 17D-F showed the enhancement of uIPSCs responding both to

1 μM acetylcholine and to 1 μM nicotine. Acetylcholine increased the uIPSC amplitude from 94.4 ± 33.9 pA to 109.4 ± 35.6 pA in FS→MS connections (n = 8; $P < 0.01$, paired *t*-test; Fig. 17D-F, H). The failure rate was decreased from 15.4 ± 6.1% to 7.4 ± 4.6%, n = 8; $P < 0.05$, Wilcoxon test) and the PPR was also decreased from 0.72 ± 0.05 to 0.58 ± 0.04 (n = 8; $P < 0.05$, paired *t*-test; Fig. 17D-F, H).

These results suggest that the endogenous cholinergic agonist, acetylcholine, induces the contradictory effects on uIPSCs in MS→MS and FS→MS connections.

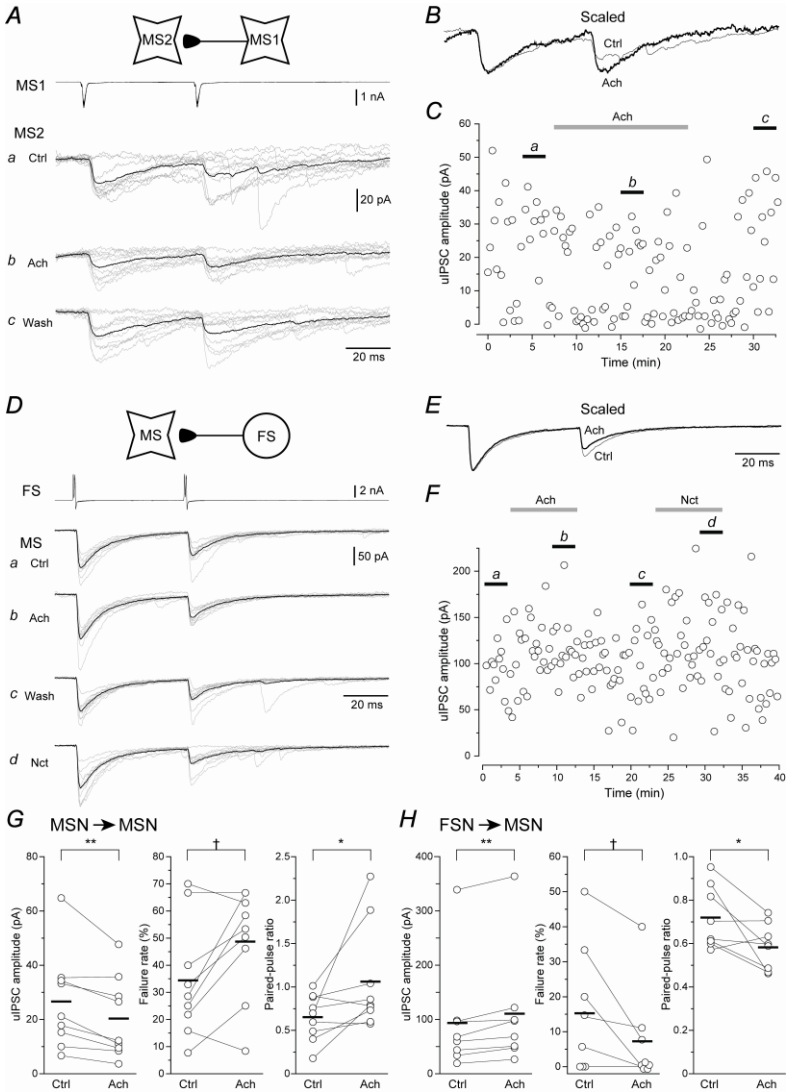

Figure 17. Effects of 1 μM acetylcholine on uIPSCs in MS→MS and FS→MS connections. **A**: Typical traces in control (Ctrl, **a**), during the application of acetylcholine (Ach, **b**), and after washing (**c**). Top traces show presynaptic action currents (MS1). Acetylcholine suppressed uIPSCs (MS2). **B**: The scaled uIPSCs in the control and during the acetylcholine application shown in **A**. Note the lesser effect of acetylcholine on the 2nd uIPSC. **C**: The time course of uIPSC amplitude on the application of acetylcholine shown in **A** and **B**. **D**: Typical traces in control (Ctrl, **a**), during the application of acetylcholine (Ach, **b**), after washing (**c**), and 1μM nicotine application (Nct, **d**). Top traces show presynaptic action currents (FS). Acetylcholine and nicotine facilitate uIPSCs. **E**: The scaled uIPSCs in the control and during the acetylcholine application shown in **D**. Note the lesser effect of acetylcholine on the 2nd uIPSC. **F**: The time course of uIPSC amplitude on the application of acetylcholine and nicotine shown in **D** and **E**. **G**: A summary of acetylcholine-induced effects on the uIPSC amplitude, the failure rate, and the paired-pulse ratio in MS→MS connections (n = 9). **H**: A summary of acetylcholine-induced effects on the uIPSC amplitude, the failure rate, and the paired-pulse ratio in FS→MS connections (n = 8). * $P < 0.05$, paired *t*-test. ** $P < 0.01$, paired *t*-test. † $P < 0.05$, Wilcoxon test.

Pilocarpine increases mIPSC frequency in the NAc medium spiny neurons

Although mIPSC recordings cannot distinguish between the presynaptic neuron subtypes of GABAergic inputs, their frequency most likely reflects GABA release from presynaptic terminals (Hirsch et al., 1999). To examine the effects of pilocarpine and nicotine on mIPSCs, spontaneous IPSCs were recorded from MS neurons under the application of 1 μM tetrodotoxin, 50 μM D-APV, and 20 μM DNQX.

Fig. 18 shows typical traces of mIPSCs recorded before and during the application of 1 μM pilocarpine. Pilocarpine reduced the frequency of mIPSCs (Fig. 18A and B). Cumulative probability plots of mIPSC interevent intervals and amplitudes were obtained from 1700 mIPSCs obtained from 17 MS neurons (100 events per neuron). The application of pilocarpine shifted the cumulative plot of the interevent interval toward the right ($P < 0.01$, K-S test), indicating that the interevent interval of mIPSCs increased due to pilocarpine treatment (Fig. 18C). Conversely, pilocarpine had little effect on the amplitude of mIPSCs ($P > 0.10$, K-S test; Fig. 18C). The mean interevent interval and the amplitude of mIPSCs were also compared between controls and neurons treated with pilocarpine. Pilocarpine increased the interevent interval from 1287.0 ± 195.1 ms to 1456.0 ± 224.9 ms (n = 17, $P < 0.05$, paired *t*-test) without affecting the mIPSC amplitude (20.3 ± 1.1 pA vs. 19.8 ± 1.2 pA; n = 17, $P > 0.2$, paired *t*-test).

In contrast to the effects of pilocarpine, nicotine (1 μM) slightly decreased the interevent interval of mIPSCs (Fig. 18D, E). The cumulative plot of the interevent interval of mIPSCs was shifted toward the left by nicotine (900 events obtained from 9 MS neurons; $P < 0.001$, K-S test) without affecting the amplitude ($P > 0.18$, K-S test; Fig. 18F). Nicotine treatment caused the mean interevent interval of mIPSCs to decrease; however, the *P* value did not reach the statistical threshold (2262.8 ± 445.1 ms to 2000.4 ± 352.0 ms, n = 9; $P > 0.05$, paired *t*-test). The mean amplitude of mIPSCs was not affected by nicotine (22.0 ± 1.9 pA to 21.3 ± 1.8 pA, n = 9; $P > 0.29$, paired *t*-test).

These findings involving mIPSCs suggest that muscarinic and nicotinic receptors reciprocally regulate the frequency of inhibitory inputs to the NAc MS neurons.

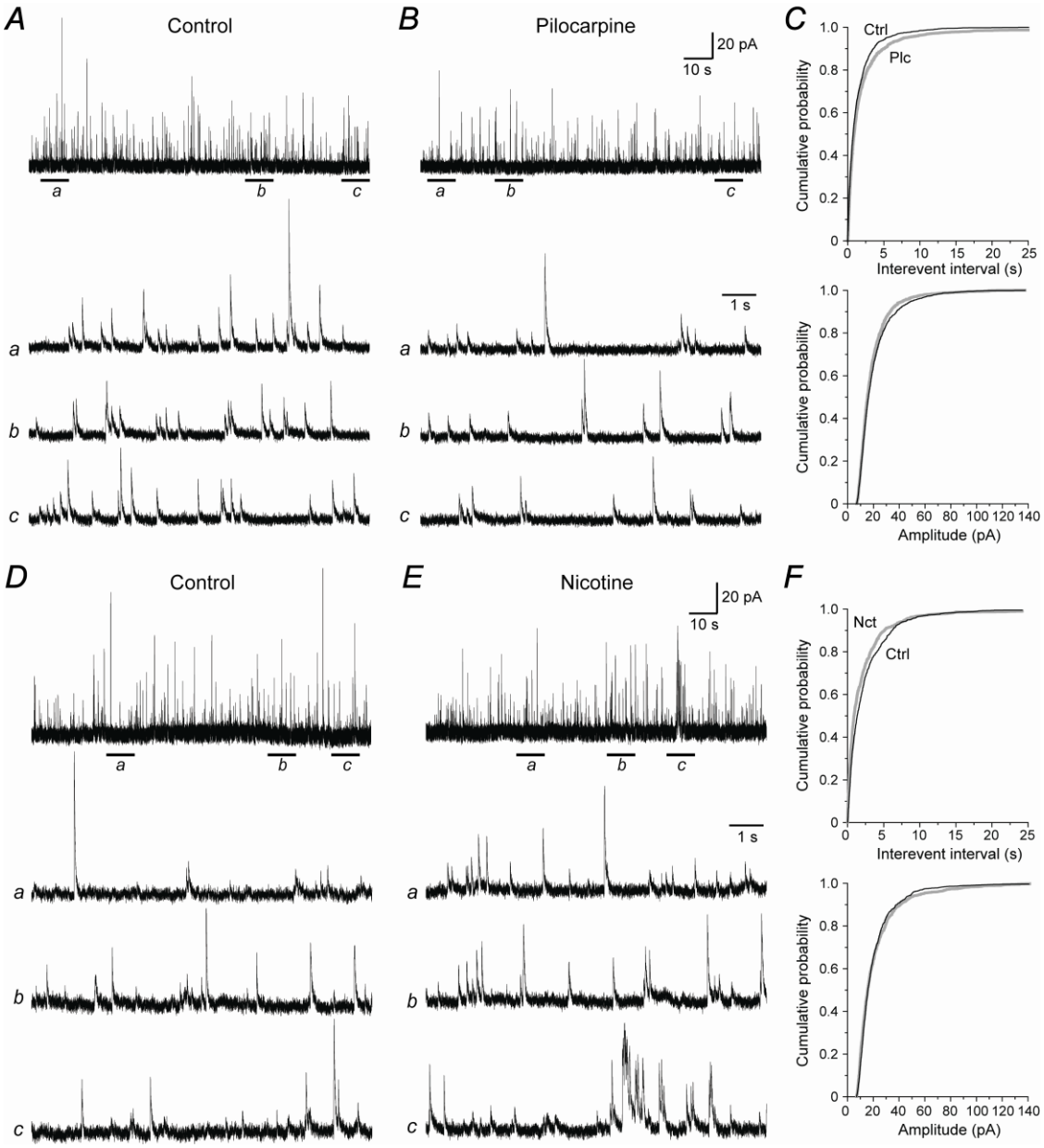

Figure 18. The effects of 1 μM pilocarpine and 1 μM nicotine on miniature IPSCs (mIPSCs) recorded from the NAc MS neurons under the application of 1 μM tetrodotoxin, 50 μM D-APV, and 20 μM DNQX. ***A*** and ***B***: An example of mIPSCs recorded before (***A***) and during the application of pilocarpine (***B***). The holding potential was set at 0 mV. Bottom panels (***a***–***c***) are time-expanded views of the regions indicated by the bars under the top trace. ***C***: Cumulative probability plots of the interevent interval (left) and the amplitude of the mIPSCs obtained from 17 MS neurons. Note that pilocarpine (gray) increased the interevent interval of mIPSCs without changing their amplitude. ***D***: An example of mIPSCs recorded before (***D***) and after the application of nicotine (***E***). Bottom panels (***a***–***c***) are time-expanded views of the regions indicated by the bars under the top trace. ***F***, Cumulative probability plots of the interevent interval (left) and the amplitude of mIPSCs obtained from 9 MS neurons. Note the leftward shift of the cumulative plot of the interevent interval caused by nicotine (gray).

Discussion

The present study demonstrated the contradictory roles of muscarinic and nicotinic receptors in the modulation of inhibitory synaptic transmission to MS neurons in the NAc shell. Specifically, muscarinic suppression of IPSCs in MS→MS connections and nicotinic facilitation of FS→MS connections were observed. Both cholinergic modulations were likely mediated via presynaptic mechanisms, such as changes in the release probability of GABA.

Muscarinic effects on uIPSCs

The muscarinic effects on GABA-mediated inhibitory synaptic transmission in the NAc or striatum have been primarily studied by recording sIPSCs and mIPSCs. Muscarinic modulation of the frequency of sIPSCs appears consistent. For example, a decrease in sIPSC frequency in the NAc was previously observed (de Rover et al., 2002; Musella et al., 2010). The decrease in sIPSC frequency was potentially induced by either postsynaptic or presynaptic mechanisms.

The activation of muscarinic receptors depolarizes MS neurons via M_1 receptors (Hsu et al., 1996; Ebihara et al., 2013). The depolarization of MS neurons triggers spike firing, which in turn increases inhibitory inputs from MS neurons to MS neurons. This postsynaptic mechanism is supported by the report that little change is induced in mIPSC frequencies and amplitudes by the activation of muscarinic receptors (de Rover et al., 2002); however, presynaptic mechanisms have also been proposed. A muscarinic M_1 agonist decreases mIPSC frequency without changing the amplitude in the striatum (Musella et al., 2010), suggesting that the suppression of GABAergic synapses by muscarinic receptors occurs presynaptically. Furthermore, the depolarization of postsynaptic MS neurons in combination with tonic activation of cholinergic interneurons causes suppression of IPSCs recorded from the MS neurons that are mediated by presynaptic CB_1 cannabinoid receptors (Narushima et al., 2007). In a previously proposed model, M_1 receptors were suggested to primarily exist in the postsynaptic MS neuron somata and dendrites (Narushima et al., 2007; Uchigashima et al., 2007).

The present results obtained from uIPSC and mIPSC recordings imply that this presynaptic mechanism may be applicable to the NAc MS→MS connections. Furthermore, the present study extended the previous findings by demonstrating that the presynaptic suppressive mechanism of GABA release via muscarinic receptors cannot be applied to FS→MS connections in the NAc. The muscarinic suppression of uIPSCs in MS→MS connections is likely to be mediated by endocannabinoid signaling at least in part (Narushima et al., 2007). However, it was considered that direct activation of the presynaptic muscarinic receptors may play a major role in the muscarinic suppression of uIPSCs, since AM251 or the postsynaptic BAPTA injection did not completely blocked the carbachol- or pilocarpine-induced uIPSC suppression.

Nicotinic facilitation of uIPSCs in FS→MS connections

In both MS→MS and FS→MS connections, nicotine and pilocarpine induced different effects in uIPSCs. MS→MS connections showed little effect of nicotine on uIPSC amplitude in contrast to the suppressive effects of pilocarpine. In contrast, FS→MS connections exhibited facilitative effects of nicotine on the uIPSC amplitude, whereas pilocarpine had little effect on these connections. These results suggest that a different cholinergic modulatory system exists between MS→MS and FS→MS connections.

Previous studies have demonstrated that the activation of nicotinic receptors increases sIPSC frequency; however, its effect on sIPSC amplitude is controversial in the NAc (de Rover et al., 2002; de Rover et al., 2005; Witten et al., 2010). de Rover et al. (2002) have previously demonstrated that nicotine causes no significant change in mIPSC frequency and

amplitude. In general, changes in the frequency of miniature events reflect the release probability from presynaptic terminals (Prange & Murphy, 1999); therefore, their study suggests that nicotine affects sIPSCs postsynaptically. In contrast, the present analysis of cumulative plots demonstrated a significant decrease in the mIPSC interevent interval, although the mean interevent interval was not significantly changed. Considering the analyses of uIPSCs, the nicotine-induced uIPSC facilitation is likely caused by presynaptic mechanisms.

A possible explanation for the discrepancy of the present miniature analyses is that the cumulative plot analysis is more sensitive than the comparison of the mean, and the slight decrease in mIPSC frequency during nicotine application cannot be detected by the latter method. The previous study demonstrated that three types of inhibitory neurons, e.g., MS neuron, FS neuron, and persistent and low-threshold spike neurons, are found in the NAc shell slice preparation, as reported in the striatum (Kawaguchi, 1993; Kohnomi et al., 2012). According to the study, the population of FS neurons is 2.2%, and the majority of the neurons found in this region are MS neurons (97.6%). Although the number of FS neuron and MS neuron synapses to an MS neuron remains unknown, it is reasonable to postulate that the major components of mIPSCs are inputs from MS neurons, which may cause the frequency of mIPSCs to be less sensitive to changes in the release probability of FS→MS connections.

Functional implications

The decrease in the amplitude of uIPSCs in MS→MS connections via muscarinic receptors suggests that suppression of the lateral inhibition occurs, which may contribute to facilitate synchronized GABAergic outputs from the NAc shell. In contrast, nicotinic facilitation of FS→MS connections likely suppresses the neural activities of MS neurons. The muscarinic and nicotinic effects on uIPSCs were mimicked by acetylcholine, and therefore, the reciprocal regulation of inhibitory synaptic transmission is also applicable to *in vivo* NAc shell. If so, it is attractive to explore how this cholinergic modulation of GABAergic synapses function *in vivo*.

Cholinergic neurons are tonically active *in vivo* (Wilson et al., 1990); therefore, acetylcholine is likely to be released spontaneously. Indeed, a recent study using optogenetic photoinhibition clearly demonstrated that the activity of inhibitory cholinergic interneurons rapidly increases repetitive spike firing in the NAc (Witten et al., 2010). Furthermore, the optogenetic study demonstrated that the activation of cholinergic interneurons abruptly inhibits spike firing. The ionotropic application of acetylcholine also inhibits spontaneous active neuron firing (Windels & Kiyatkin, 2003). In combination with the previous study that reported the muscarinic suppression of repetitive spike firing in the NAc MS neurons (Ebihara et al., 2013), cholinergic modulation moderately reduces the frequency of repetitive spike firing of the NAc MS neurons at the baseline. The nicotinic facilitation of FS→MS connections may support the suppression of MS neuron activities. In contrast, the muscarinic suppression of the lateral inhibition (MS→MS connections) may synchronize the outputs from the NAc to other structures of the basal ganglia.

This cholinergic modulation of neural activities in the NAc may be involved in pathophysiological functions, such as in cocaine (Witten et al., 2010) and amphetamine exposure (Guix et al., 1992). The relationship between drug abuse and the cholinergic system in the NAc should be further explored in the future.

CONCLUSIONS

Cholinergic interneurons in the NAc modulate neural functions of MS and FS neurons. Multiple whole-cell patch-clamp recordings were performed to examine the cholinergic roles in (1) repetitive firing properties of MS neurons, and (2) uIPSCs between MS→MS and FS→MS connections.

Bath application of carbachol increased rheobase, which delayed the action potential initiation of MS neurons. These cholinergic effects were mimicked by eliciting action potentials in cholinergic interneurons. uIPSCs recorded from MS→MS connections were suppressed by activation of muscarinic receptors, whereas FS→MS connections were facilitated by nicotinic receptor activation.

Taken together with these findings, it is concluded that, (1) muscarinic receptors suppress suprathreshold responses of MS neurons and lateral inhibition in the NAc, and (2) nicotinic receptors suppress MS neural activities by potentiating the inhibition from FS neurons (Fig. 19).

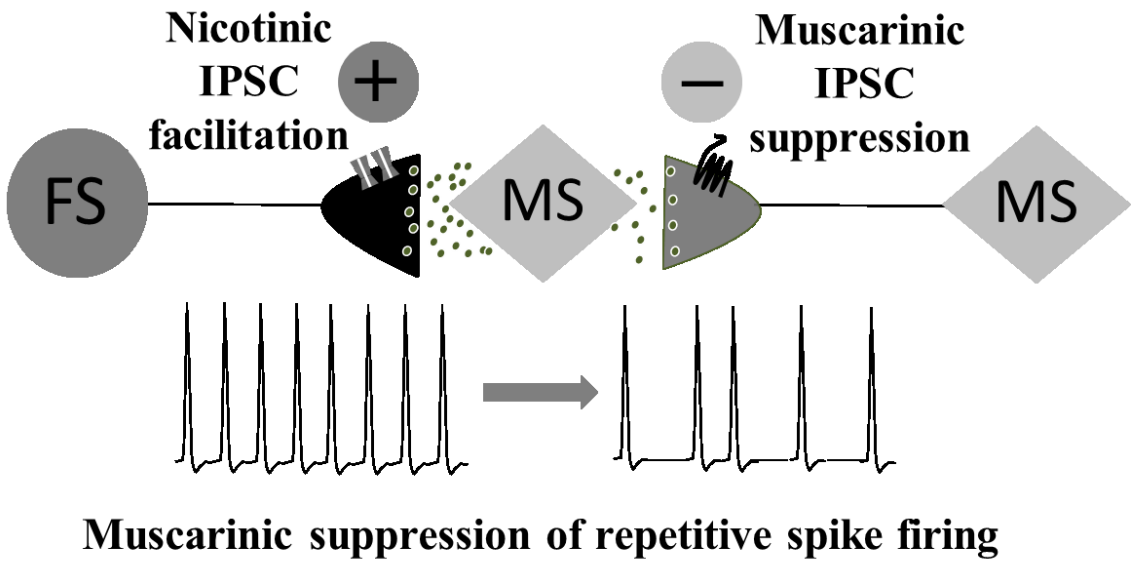

Figure 19. Proposed mechanisms of cholinergic modulation of MS firing properties and inhibitory synaptic transmission in the NAc shell. uIPSCs are suppressed by activation of muscarinic receptors in MS→MS connections and are facilitated via nicotinic receptors in FS→MS connections. Activation of MS muscarinic receptors reduces suprathreshold spike firing frequency of MS neurons.

ACKNOWLEDGMENTS

I thank to Profs. Koichiro Ueda and Noriaki Koshikawa for editing the manuscript, and to Dr. Masayuki Kobayashi for instruction of experiments and editing the manuscript. I also appreciate Profs. Yuchio Yanagawa, Yasuo Kawaguchi and Masumi Hirabayashi for providing VGAT-Venus transgenic rats.

This work was supported by JSPS KAKENHI 23890216 to Kiyofumi Yamamoto, JSPS KAKENHI 24659831 to Masayuki Kobayashi and JSPS KAKENHI 25293379 to Masayuki Kobayashi from the Japanese Ministry of Education, Culture, Sports, Science and Technology; a Nihon University Joint Grant Research Grant to Masayuki Kobayashi; the Promotion and Mutual Aid Corporation for Private Schools of Japan to Yuko Koyanagi, Noriaki Koshikawa, and Masayuki Kobayashi; a grant for the Promotion of Multidisciplinary Research Projects entitled 'Translational Research Network on Orofacial Neurological Disorders' from the Japanese Ministry of Education, Culture, Sports, Science and Technology to Noriaki Koshikawa and Masayuki Kobayashi; and grants from the Sato and Uemura Foundations to Masayuki Kobayashi.

A part of this work has been presented in the 64th annual meeting of Nihon University Society of Dentistry (May 20, 2012; Tokyo), the 36th Annual Meeting of the Japan Neuroscience Society (June 20-23, 2013; Kyoto), and Neuroscience 2013 (November 9-13, 2013; San Diego). This work received Young Investigation Award of the Nihon University Society of Dentistry.

REFERENCES

Akaike A, Sasa M, Takaori S. Muscarinic inhibition as a dominant role in cholinergic regulation of transmission in the caudate nucleus. *J Pharmacol Exp Ther* 246: 1129-1136, 1988.

Akins PT, Surmeier DJ, Kitai ST. Muscarinic modulation of a transient K^+ conductance in rat neostriatal neurons. *Nature* 344: 240-242, 1990.

Bacci A, Rudolph U, Huguenard JR, Prince DA. Major differences in inhibitory synaptic transmission onto two neocortical interneuron subclasses. *J Neurosci* 23: 9664-9674, 2003.

Calabresi P, Centonze D, Gubellini P, Pisani A, Bernardi G. Blockade of M2-like muscarinic receptors enhances long-term potentiation at corticostriatal synapses. *Eur J Neurosci* 10: 3020-3023, 1998.

Calabresi P, Centonze D, Gubellini P, Pisani A, Bernardi G. Acetylcholine-mediated modulation of striatal function. *Trends Neurosci* 23: 120-126, 2000.

Chen G, Kittler JT, Moss SJ, Yan Z. Dopamine D_3 receptors regulate $GABA_A$ receptor function through a phospho-dependent endocytosis mechanism in nucleus accumbens. *J Neurosci* 26: 2513-2521, 2006.

Contant C, Umbriaco D, Garcia S, Watkins KC, Descarries L. Ultrastructural characterization of the acetylcholine innervation in adult rat neostriatum. *Neuroscience* 71: 937-947, 1996.

Cools AR, Miwa Y, Koshikawa N. Role of dopamine D_1 and D_2 receptors in the nucleus accumbens in jaw movements of rats: a critical role of the shell. *Eur J Pharmacol* 286: 41-47, 1995.

de Rover M, Lodder JC, Kits KS, Schoffelmeer AN, Brussaard AB. Cholinergic modulation of nucleus accumbens medium spiny neurons. *Eur J Neurosci* 16: 2279-2290, 2002.

de Rover M, Lodder JC, Schoffelmeer AN, Brussaard AB. Intermittent morphine treatment induces a long-lasting increase in cholinergic modulation of GABAergic synapses in nucleus accumbens of adult rats. *Synapse* 55: 17-25, 2005.

de Rover M, Lodder JC, Smidt MP, Brussaard AB. Pitx3 deficiency in mice affects cholinergic modulation of GABAergic synapses in the nucleus accumbens. *J Neurophysiol* 96: 2034-2041, 2006.

Di Chiara G. Nucleus accumbens shell and core dopamine: differential role in behavior and addiction. *Behav Brain Res* 137: 75-114, 2002.

Dodt HU, Misgeld U. Muscarinic slow excitation and muscarinic inhibition of synaptic transmission in the rat neostriatum. *J Physiol* 380: 593-608, 1986.

Ebihara K, Yamamoto K, Ueda K, Koshikawa N, Kobayashi M. Cholinergic interneurons suppress action potential initiation of medium spiny neurons in rat nucleus accumbens shell. *Neuroscience* 236: 332-344, 2013.

English DF, Ibanez-Sandoval O, Stark E, Tecuapetla F, Buzsáki G, Deisseroth K, Tepper JM, Koos T. GABAergic circuits mediate the reinforcement-related signals of striatal cholinergic interneurons. *Nat Neurosci* 15: 123-130, 2012.

Gabel LA, Nisenbaum ES. Muscarinic receptors differentially modulate the persistent potassium current in striatal spiny projection neurons. *J Neurophysiol* 81: 1418-1423, 1999.

Galarraga E, Hernandez-Lopez S, Reyes A, Miranda I, Bermudez-Rattoni F, Vilchis C, Bargas J. Cholinergic modulation of neostriatal output: a functional antagonism between different types of muscarinic receptors. J Neurosci 19:3629-3638, 1999.

Gertler TS, Chan CS, Surmeier DJ. Dichotomous anatomical properties of adult striatal medium spiny neurons. *J Neurosci* 28: 10814-10824, 2008.

Groenewegen HJ, Berendse HW, Meredith GE, Haber SN, Voorn P, Wolters JG, Lohman AH. *Functional anatomy of the ventral, limbic system-innervated striatum*. John Wiley and Sons, New York, 1991.

Guix T, Hurd YL, Ungerstedt U. Amphetamine enhances extracellular concentrations of dopamine and acetylcholine in dorsolateral striatum and nucleus accumbens of freely moving rats. *Neurosci Lett* 138: 137-140, 1992.

Gulley JM, Doolen S, Zahniser NR. Brief, repeated exposure to substrates down-regulates dopamine transporter function in Xenopus oocytes in vitro and rat dorsal striatum in vivo. *J Neurochem* 83: 400-411, 2002.

Hirsch JC, Agassandian C, Merchán-Pérez A, Ben-Ari Y, DeFelipe J, Esclapez M, Bernard C. Deficit of quantal release of GABA in experimental models of temporal lobe epilepsy. *Nat Neurosci* 2: 499-500, 1999.

Hopf FW, Cascini MG, Gordon AS, Diamond I, Bonci A. Cooperative activation of dopamine D_1 and D_2 receptors increases spike firing of nucleus accumbens neurons via G-protein βγ subunits. *J Neurosci* 23: 5079-5087, 2003.

Hsu KS, Huang CC, Gean PW. Muscarinic depression of excitatory synaptic transmission mediated by the presynaptic M3 receptors in the rat neostriatum. *Neurosci Lett* 197: 141-144, 1995.

Hsu KS, Yang CH, Huang CC. Carbachol induces inward current in rat neostriatal neurons through a G-protein-coupled mechanism. *Neurosci Lett* 224: 79-82, 1997.

Hsu KS, Yang CH, Huang CC, Gean PW. Carbachol induces inward current in neostriatal neurons through M_1-like muscarinic receptors. *Neuroscience* 73: 751-760,1996.

Jiang L, Sun S, Nedergaard M, Kang J. Paired-pulse modulation at individual GABAergic synapses in rat hippocampus. *J Physiol* 523 Pt 2: 425-439, 2000.

Kawaguchi Y. Physiological, morphological, and histochemical characterization of three classes of interneurons in rat neostriatum. *J Neurosci* 13: 4908-4923, 1993.

Kawaguchi Y, Wilson CJ, Augood SJ, Emson PC. Striatal interneurones: chemical, physiological and morphological characterization. *Trends Neurosci* 18: 527-535, 1995.

Kitamura M, Koshikawa N, Yoneshige N, Cools AR. Behavioural and neurochemical effects of cholinergic and dopaminergic agonists administered into the accumbal core and shell in rats. *Neuropharmacology* 38: 1397-1407, 1999.

Kobayashi M, Takei H, Yamamoto K, Hatanaka H, Koshikawa N. Kinetics of $GABA_B$ autoreceptor-mediated suppression of GABA release in rat insular cortex. *J Neurophysiol* 107: 1431-1442, 2012.

Kohnomi S, Koshikawa N, Kobayashi M. D_2-like dopamine receptors differentially regulate unitary IPSCs depending on presynaptic GABAergic neuron subtypes in rat nucleus accumbens shell. *J Neurophysiol* 107: 692-703, 2012.

Koshikawa N, Koshikawa F, Tomiyama K, Kikuchi de Beltrán K, Kamimura F, Kobayashi M. Effects of dopamine D_1 and D_2 agonists and antagonists injected into the nucleus accumbens and globus pallidus on jaw movements of rats. *Eur J Pharmacol* 182: 375-380, 1990.

Lin JY, Chung KK, de Castro D, Funk GD, Lipski J. Effects of muscarinic acetylcholine receptor activation on membrane currents and intracellular messengers in medium spiny neurones of the rat striatum. *Eur J Neurosci* 20: 1219-1230, 2004.

Ma YY, Cepeda C, Chatta P, Franklin L, Evans CJ, Levine MS. Regional and cell-type-specific effects of DAMGO on striatal D1 and D2 dopamine receptor-expressing medium-sized spiny neurons. *ASN Neuro* 4: e00077, 2012.

Musella A, De Chiara V, Rossi S, Cavasinni F, Castelli M, Cantarella C, Mataluni G, Bernardi G, Centonze D. Transient receptor potential vanilloid 1 channels control acetylcholine/2-arachidonoylglicerol coupling in the striatum. *Neuroscience* 167: 864-871, 2010.

Narushima M, Uchigashima M, Fukaya M, Matsui M, Manabe T, Hashimoto K, Watanabe M, Kano M. Tonic enhancement of endocannabinoid-mediated retrograde suppression of inhibition by cholinergic interneuron activity in the striatum. *J Neurosci* 27: 496-506, 2007.

Nicola SM. The nucleus accumbens as part of a basal ganglia action selection circuit. *Psychopharmacology (Berl)* 191: 521-550, 2007.

Nicola SM, Malenka RC. Dopamine depresses excitatory and inhibitory synaptic transmission by distinct mechanisms in the nucleus accumbens. *J Neurosci* 17: 5697-5710, 1997.

Nicola SM, Malenka RC. Modulation of synaptic transmission by dopamine and norepinephrine in ventral but not dorsal striatum. *J Neurophysiol* 79: 1768-1776, 1998.

Nisenbaum ES, Wilson CJ. Potassium currents responsible for inward and outward rectification in rat neostriatal spiny projection neurons. *J Neurosci* 15: 4449-4463, 1995.

Pakhotin P, Bracci E. Cholinergic interneurons control the excitatory input to the striatum. *J Neurosci* 27: 391-400, 2007.

Pennartz CM, Groenewegen HJ, Lopes da Silva FH. The nucleus accumbens as a complex of functionally distinct neuronal ensembles: an integration of behavioural, electrophysiological and anatomical data. *Prog Neurobiol* 42: 719-761, 1994.

Pennartz CM, Kitai ST. Hippocampal inputs to identified neurons in an in vitro slice preparation of the rat nucleus accumbens: evidence for feed-forward inhibition. *J Neurosci* 11: 2838-2847, 1991.

Perez-Rosello T, Figueroa A, Salgado H, Vilchis C, Tecuapetla F, Guzman JN, Galarraga E, Bargas J. Cholinergic control of firing pattern and neurotransmission in rat neostriatal projection neurons: role of CaV2.1 and CaV2.2 Ca^{2+} channels. *J Neurophysiol* 93: 2507-2519, 2005.

Phelps PE, Houser CR, Vaughn JE. Immunocytochemical localization of choline acetyltransferase within the rat neostriatum: a correlated light and electron microscopic study of cholinergic neurons and synapses. *J Comp Neurol* 238: 286-307, 1985.

Prange O, Murphy TH. Correlation of miniature synaptic activity and evoked release probability in cultures of cortical neurons. *J Neurosci* 19: 6427-6438, 1999.

Ridray S, Griffon N, Mignon V, Souil E, Carboni S, Diaz J, Schwartz JC, Sokoloff P. Coexpression of dopamine D_1 and D_3 receptors in islands of Calleja and shell of nucleus accumbens of the rat: opposite and synergistic functional interactions. *Eur J Neurosci* 10: 1676-1686, 1998.

Rymar VV, Sasseville R, Luk KC, Sadikot AF. Neurogenesis and stereological morphometry of calretinin-immunoreactive GABAergic interneurons of the neostriatum. *J Comp Neurol* 469: 325-339, 2004.

Sharp T, Zetterstrom T, Ljungberg T, Ungerstedt U. A direct comparison of amphetamine-induced behaviours and regional brain dopamine release in the rat using intracerebral dialysis. *Brain Res* 401: 322-330, 1987.

Shen W, Hamilton SE, Nathanson NM, Surmeier DJ. Cholinergic suppression of KCNQ channel currents enhances excitability of striatal medium spiny neurons. *J Neurosci* 25: 7449-7458, 2005.

Shinonaga Y, Takada M, Mizuno N. Topographic organization of collateral projections from the basolateral amygdaloid nucleus to both the prefrontal cortex and nucleus accumbens in the rat. *Neuroscience* 58: 389-397, 1994.

Stevens CF, Wang Y. Facilitation and depression at single central synapses. *Neuron* 14: 795-802, 1995.

Stuber GD, Hnasko TS, Britt JP, Edwards RH, Bonci A. Dopaminergic terminals in the nucleus accumbens but not the dorsal striatum corelease glutamate. *J Neurosci* 30: 8229-8233, 2010.

Sugita S, Uchimura N, Jiang ZG, North RA. Distinct muscarinic receptors inhibit release of γ-aminobutyric acid and excitatory amino acids in mammalian brain. *Proc Natl Acad Sci U S A* 88: 2608-2611, 1991.

Takagi M, Yamamoto C. Suppressing action of cholinergic agents on synaptic transmissions in the corpus striatum of rats. *Exp Neurol* 62: 433-443, 1978.

Takei H, Fujita S, Shirakawa T, Koshikawa N, Kobayashi M. Insulin facilitates repetitive spike firing in rat insular cortex via phosphoinositide 3-kinase but not mitogen activated protein kinase cascade. *Neuroscience* 170: 1199-1208, 2010.

Taverna S, Canciani B, Pennartz CM. Dopamine D1-receptors modulate lateral inhibition between principal cells of the nucleus accumbens. *J Neurophysiol* 93: 1816-1819, 2005.

Taverna S, Canciani B, Pennartz CM. Membrane properties and synaptic connectivity of fast-spiking interneurons in rat ventral striatum. *Brain Res* 1152: 49-56, 2007.

Taverna S, Ilijic E, Surmeier DJ. Recurrent collateral connections of striatal medium spiny neurons are disrupted in models of Parkinson's disease. *J Neurosci* 28: 5504-5512, 2008.

Taverna S, van Dongen YC, Groenewegen HJ, Pennartz CM. Direct physiological evidence for synaptic connectivity between medium-sized spiny neurons in rat nucleus accumbens in situ. *J Neurophysiol* 91: 1111-1121, 2004.

Threlfell S, Cragg SJ. Dopamine signaling in dorsal versus ventral striatum: the dynamic role of cholinergic interneurons. *Front Syst Neurosci* 5: 11, 2011.

Uchigashima M, Narushima M, Fukaya M, Katona I, Kano M, Watanabe M. Subcellular arrangement of molecules for 2-arachidonoyl-glycerol-mediated retrograde signaling and its physiological contribution to synaptic modulation in the striatum. *J Neurosci* 27: 3663-3676, 2007.

Uchimura N, Cherubini E, North RA. Inward rectification in rat nucleus accumbens neurons. *J Neurophysiol* 62: 1280-1286, 1989.

Uematsu M, Hirai Y, Karube F, Ebihara S, Kato M, Abe K, Obata K, Yoshida S, Hirabayashi M, Yanagawa Y, Kawaguchi Y. Quantitative chemical composition of cortical GABAergic neurons revealed in transgenic venus-expressing rats. *Cereb Cortex* 18: 315-330, 2008.

Wilson CJ, Chang HT, Kitai ST. Firing patterns and synaptic potentials of identified giant aspiny interneurons in the rat neostriatum. *J Neurosci* 10: 508-519, 1990.

Windels F, Kiyatkin EA. Modulatory action of acetylcholine on striatal neurons: microiontophoretic study in awake, unrestrained rats. *Eur J Neurosci* 17: 613-622, 2003.

Witten IB, Lin SC, Brodsky M, Prakash R, Diester I, Anikeeva P, Gradinaru V, Ramakrishnan C, Deisseroth K. Cholinergic interneurons control local circuit activity and cocaine conditioning. *Science* 330: 1677-1681, 2010.

Yamamoto K, Ebihara K, Koshikawa N, Kobayashi M. Reciprocal regulation of inhibitory synaptic transmission by nicotinic and muscarinic receptors in rat nucleus accumbens shell. *J Physiol* 591: 5745-5763, 2013

Zhang L, Warren RA. Muscarinic and nicotinic presynaptic modulation of EPSCs in the nucleus accumbens during postnatal development. *J Neurophysiol* 88: 3315-3330, 2002.

Zhou FM, Wilson C, Dani JA. Muscarinic and nicotinic cholinergic mechanisms in the mesostriatal dopamine systems. *Neuroscientist* 9: 23-36, 2003.